MSc Mini-Dissertation

Modelling of fission product release from TRISO fuel during accident conditions: Benchmark code comparison

Student: Alastair Ramlakan

Supervisor: Prof. Eben Mulder

Co-Supervisor: Dr. Hanno van der Merwe

ABSTRACT

This document gives an overview of the proposed MSc study. The main goal of the study is to model the cases listed in the code benchmark study of the International Atomic Energy Agency CRP-6 fuel performance study (Verfondern & Lee, 2005).

The platform that will be employed is the GETTER code (Keshaw & van der Merwe, 2006). GETTER was used at PBMR for the release calculations of metallic and some non-metallic long-lived fission products. GETTER calculates the transport of fission products from their point of fission to release from the fuel surface taking into account gas precursors and activation products.

Results show that for certain experiments the codes correspond very well with the experimental data whilst in others there are orders of magnitude differences. It can be seen that very similar behaviour is observed in all codes. Improvements are needed in updating the strontium diffusion coefficient and in understanding, on a deeper level, the transport of silver in TRISO particles and how it deviates from simple diffusion models.

CONTENTS

FIGURES

Abbreviations

The following list contains the abbreviations used in this document.

Abbreviation or Acronym	Definition
CCCTF	Core Conduction Cooldown Test Facility
CFD	Computational Fluid Dynamics
CRP	Coordinated Research Project
EFPD	Effective Full Power Days
EUO	Enriched Uranium Dioxide
FIMA	Fissions per Initial Metal Atom
GA	General Atomics
GLE	Pressed Low Enriched
HEU	High Enriched Uranium
HFR	High Flux Reactor
HTR	High Temperature Gas Cooled Reactor
IAEA	International Atomic Energy Agency
INL	Idaho National Laboratories
LEU	Low Enriched Uranium
LWR	Light Water Reactor
MCNP	Monte Carlo N Particle
PBR	Pebble Bed Reactor
PBMR	Pebble Bed Modular Reactor
PBMR (Pty) Ltd	Pebble Bed Modular Reactor (Pty) Ltd
PyC	PyroCarbon
SiC	Silicon Carbide
TRISO	Tristructural-isotropic

Abbreviation or Acronym	Definition
UC	Uranium Carbide
UCO	Uranium Oxicarbide
UO	Uranium Oxide
VSOP	Very Superior Old Program

1. Introduction

1.1 *Background*

High Temperature Gas Cooled Reactor (HTR) Technology (O'Connor, 2009) has, in the past decade, become a subject area of renewed research interest due to the recent nuclear renaissance as a result of a need to lower CO_2 emissions whilst being able to meet an increasing worldwide demand for energy in the form of electricity, process heat generation and hydrogen production.

The advantages of HTRs is that their inherent safety features make events leading to severe core damage highly unlikely and constitute the main differentiating aspects compared to LWRs.

To retain fission products after postulated accidents, power reactors usually rely on active safety systems inside the primary circuit, such as redundant shut down systems and multiple redundant decay heat removal systems. The HTR reactor is designed to handle high temperatures, has a low power density, can cool by natural circulation and passive means without active safety systems and remain intact in accident scenarios which may raise the temperature of the reactor to 1600°C.

1.2 *CRP-6 Benchmark Exercise*

The overall objectives of IAEA CRP-6 (Verfondern & Lee, 2005) are:

- Support the development of improved HTR fuel technology;
- Facilitate the coordination of technology development activities; and
- Exchange relevant technical information among the interested Member States.

Fuel performance benchmarks, in aid of model V&V, are a subtask under IAEA CRP-6 for normal operation and accident conditions and consist of the following parts:

1. Simple calculation cases to verify the code and its submodels.
2. Validation via postcalculation of well-documented irradiation/heating experiments.
3. Prediction of fuel performance in future experiments.

Table 1: CRP-6 Participants and Codes Used

Country	Code
France	ATLAS (Phelip et al., 2004)
Germany	FRESCO (Krohn and Finken, 1983)
Korea	COPA (Kim & Cho, 2008)
South Africa	GETTER (Rollig, 2001, Keshaw & van der Merwe, 2006)
USA (INL)	PARFUME (Miller et al., 2004)
USA (GA)	PISA / CAPPER (Richards, 1993)

Other countries, such as Russia and the United Kingdom may have submitted results but these were not available at time of writing.

1.2.1 Sensitivity Study

The sensitivity study involves modelling a bare kernel, a kernel with a PyC layer and single TRISO particles, both intact and with defects. Irradiation parameters and accident conditions are varied to examine their influence on the failure probability of fuel particles. These simple cases are used for validation purposes.

1.2.2 Past Experiments

Several irradiation and heating experiments have been evaluated. These were the HFR-K3/1, HFR-K3/3, HFR-P4/1-12, HFR-P4/3-7 and HFR-K6/3 which were part of the German HTR experimental programme. The fuel spheres were irradiated in the HFR Petten reactor and heatup tests were performed in the KUEFA furnace at the Research Centre Jülich.

Japanese fuel was irradiated in the HRB-22 irradiation experiment and heatup was performed at the US Core Conduction Cooldown Test Facility.

1.2.3 Future Experiments

The two planned experiments used were the HFR-EU1bis and HTR-PM experiments.

2. Literature Review

2.1 *History of High Temperature Gas Cooled Reactors*

There exist two types of High Temperature Gas Cooled Reactors (NERAC & GEN IV, 2002); a prismatic block type reactor and a Pebble Bed Reactor (PBR) which both use helium as the coolant gas. In the case of prismatic block reactors the TRISO particles are contained in fuel rods which are placed within the holes of a graphite moderator block, whereas in the pebble bed case the TRISO particles are embedded within a graphite sphere. TRISO particles are

considered to retain fission products up to a temperature of approximately 1600°C, a temperature limit which is achieved by lowering the power density and thus ensuring that decay heat is removed by passive mechanisms such as natural convection and radiation (Stawicki, 2006).

The material used for core structures and the fuel matrix is graphite due to its ability to maintain its integrity and performance at high operating temperatures. Pebbles are continuously circulated in Pebble Bed Reactors based on whether they are below the burnup limit (Koster et al, 2004). Thus, no excess reactivity is needed for burnup compensation which contributes to the inherent safety of the reactor (van der Merwe, 2004).

The first High Temperature Gas Cooled Reactor built was the 20 MWe Dragon reactor in the United Kingdom which was a prismatic block type reactor (Carré et al., 2009). This was followed in the US by the 40 MWe Peach Bottom reactor (Everett & Kohler, 1978) and the 330MWe Fort St. Vrain reactor (Bramblett et al, 1980) which was the first HTR used for electricity production, operating between 1979 and 1989. Germany focused on the pebble bed-type reactors instead and built and successfully ran the 15 MWe AVR reactor from 1966 to 1987 (Ziermann, 1990). The 300 MWe Thorium High Temperature Reactor, (Schwarz, 1988) used thorium as fuel but endured technical difficulties and was shut down after only a few years.

At present the Pebble Bed Modular Reactor program in South Africa has been put into a care and maintenance program (Power Engineering International, 2010) but China is still on track with its plans of building a Pebble Bed Reactor (Next Big Future, 2010). Block type reactors are being researched and designed by General Atomics in the United States, MINATOM in Russia, Framatome in France, and Fuji Electric in Japan (Stawicki, 2006).

2.2 *TRISO Fuel Description*

Tristructural-isotropic (TRISO) fuel is used in HTRs due to its ability to maintain its integrity at temperatures up to and possibly beyond 1600°C.

The first coated particle was invented by Roy Huddle in 1957 (Verfondern, 2007). Until the establishment of SiC TRISO fuel with metal oxide or a carbide spherical kernel as the accepted HTR fuel particle, numerous different fuel particle types were experimented with. The kernels were composed of uranium monocarbide, uranium dicarbide, uranium dicarbide/thorium dicarbide, uranium monocarbide/zirconium monocarbide, or uranium dioxide, all of which were initially uncoated and later coated with different combinations of pyrocarbon and SiC.

SiC TRISO fuel particles today consist of the following layers (Verfondern, Nabielek and Kendall, 2007). The fuel kernel is either UC or UCO which is then coated with four layers which, from inside to out, are a porous carbon buffer layer, a dense inner layer of pyrolytic carbon (PyC), a ceramic layer of SiC which acts as the main barrier and finally a dense outer layer of PyC.

The SiC structure of the TRISO fuel particle is used for LEU or HEU and for both pebble and prismatic type reactors. Acceptance standards for manufacturing have made an improvement from an initial free heavy metal fraction of approximate 1E-03 to 1E-04 in the 1970's to today's requirements of at least 1E-05 (Adams, 1988). Similar standards apply for particle failure fractions.

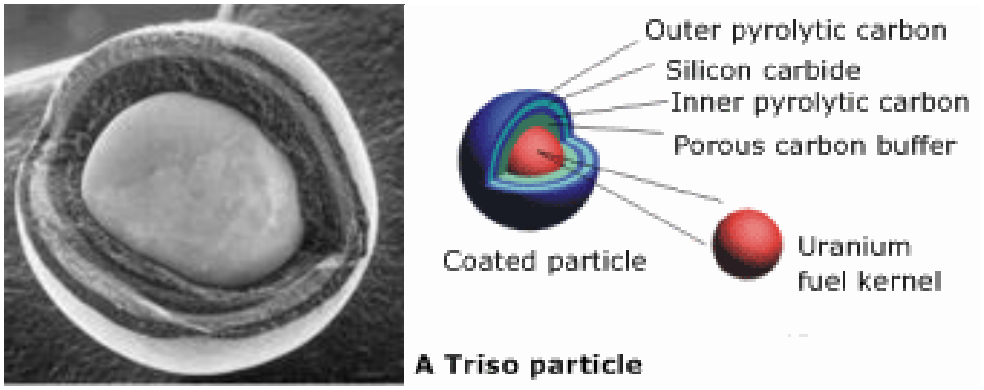

Figure 1: TRISO Particle

2.3 *TRISO Fuel Failure Mechanisms*

Miller (2001) describes the different particle failure mechanisms:

2.3.1 The Impact of Irradiation on Pyrocarbon layers

Irradiation causes swelling of the kernel and shrinking of the buffer layer which decreases the volume in the buffer layer available for storage of fission gasses. The PyC layer shrinks in both the radial and tangential direction at different rates potentially resulting in the PyC layer cracking and de-bonding at the inner PyC/SiC interface.

2.3.2 Kernel Migration

Kernel migration is the movement of the kernel toward the inner PyC layer in the presence of a temperature gradient which can result in failure of the particle. Due to higher temperature gradients in prismatic cores this phenomenon is more relevant to prismatic cores than for pebble bed type reactors.

2.3.3 Fission Product Attack

Fission products released during irradiation can migrate through the inner PyC layer whereupon they can interact with the SiC layer and cause failure of the layer. Palladium is the main fission product of concern whilst some of the rare earths may also create issues. The migration of the fission products is thought to be a function of time, temperature and burnup as well as temperature gradient, leading to its importance being higher in prismatic reactors.

2.3.4 Pressure Vessel Failure

Pressure buildup in the porous buffer layer occurs during irradiation due to the production of fission gases and CO gas. The particle layers are designed to handle large pressures but any particles with possible manufacturing defects may fail during the pressure buildup if pressures increase beyond a certain pressure. During irradiation, fission gases are released from the kernel into the porous buffer layer.

2.4 *Fission Product Transport*

2.4.1 Transport Mechanisms

HTR's are inherently safe with respect to core meltdown but still need to be shown to be safe in terms of fission product release outside the reactor building after a Loss of Coolant Accident (LOCA). For an HTR the primary barrier in terms of fission product retention is the fuel, more specifically the TRISO particle (Rollig, 1977), and thus it needs to be shown that the TRISO particle retains its integrity during the reactor operation and that reactor conditions are kept within the ranges specified by the fuel design qualification.

There are three distinct and independent sources of fission product release from fuel elements (IAEA, 2010). The fission product transport route is shown graphically in Figure 2.

1. Diffusion of fission products through the matrix material from uranium and thorium contamination of the fuel material, mainly in the matrix material of the fuel element.
2. Fission product release from defective and failed coated particles which escape the kernel, bypass the coating layers and diffuse through the matrix material.
3. Fission products from intact TRISO-particles have to be transported through all the coating layers before they can diffuse through the matrix material. Due to the fact that diffusion parameters through the coating layers are very small and thus transport rates are slow, only long-lived metallic fission products are considered for this mechanism.

Due to fission products having high kinetic energies from fission they travel a certain distance before coming to rest. Thus, fission products formed near the surface of a fuel kernel can be

released directly into the buffer region, fission products in the matrix can escape the grains directly without diffusion, fission products formed in the outer pyrocarbon layer can escape directly from the coating layer and fission products formed in the outer fuel-free zone of the spherical fuel can escape the fuel element without diffusion.

2.4.2 Transport Modelling

The transport of fission metals through fuel materials is modelled as a transient diffusion process solved numerically using appropriate boundary and interface conditions (Hanson, 2004). To model the transport by Fick's law (Nabielek, 1974) effective diffusion coefficients are used which cover a combination of migration processes such as lattice, grain boundary and pore diffusion complicated by effects like irradiation-enhanced trapping and adsorption.

To further complicate the modelling it is to be noted that the chemical speciation of fission products in the kernel changes with burnup due to changes in the oxygen potential which may have an effect on the respective transport parameters (IAEA, 2010).

Fick's first law is based on the assumption that in regions with concentration gradients of fission products, the mass flux can be related to the concentration gradient. In 1-D, it is given by (Crank, 1975)::

$$J_x = -D\frac{dc}{dx}$$

with

J_x the flux of the fission product species in the x - direction

D the diffusion coefficient of the fission product

c(x) the concentration gradient of the fission product

We also have the mass balance equation which states that the change in concentration of fission products in a control volume per unit time is equal to the net flux in or out of the control volume per unit length:

$$\frac{\partial c}{\partial t} = -\frac{\partial J}{\partial x}$$

The expression for the diffusion flux *J* in Fick's first law can be substituted in the balance equation to give us Fick's second law. Fick's second law of diffusion describes the time dependence of the concentration field on diffusion processes:

$$\frac{\partial c}{\partial t} = D\frac{\partial^2 c}{\partial x^2}$$

Taking into account the fission source *S* and radioactive decay *λc* the diffusion equation extends to:

$$\frac{\partial c}{\partial t} = D\frac{\partial^2 c}{\partial x^2} - \lambda c + S$$

with

S the fission source

λ radioactive decay constant

Converting to spherical coordinates we obtain:

$$\frac{\partial c}{\partial t} = D\left(\frac{\partial^2 c}{\partial r^2} + \frac{2}{r}\frac{\partial c}{\partial r}\right) - \lambda c + S$$

With boundary conditions:

1. The concentration gradient is 0 at $r = 0$. This is due to the fact that peak concentration occurs at the centre of the pebble and that the pebble is radially symmetric. Thus, we have:

$$\frac{\partial c}{\partial r}|_{r=0} = 0$$

2. Continuity at the interface between two adjacent materials with diffusion constants D_1, and D_2 gives:

$$D_1\frac{\partial c}{\partial r}\bigg| = D_2\frac{\partial c}{\partial r}\bigg|$$

3. For metallic fission products, an evaporative boundary condition at the fuel surface in the form of a sorption isotherm is used, relating the concentration in the matrix at the surface to the vapour pressure in the helium. Sorption isotherms for Cs, Sr and Ag for different nuclear graphites and matrix materials are presented in Verfondern (1997). Usually a Henrian isotherm (linear correlation) or a Freundlich isotherm (exponential correlation) is used.

2.4.3 Diffusion Coefficients

Effective diffusion coefficients are used in codes such as GETTER to take into account spatial inhomogeneity and temperature dependence.

The Arrhenius equation is used to take into account the temperature dependence of diffusion as the frequency of collisions between fission products is dependent on the temperature:

$$D = D_0 e^{-\frac{Q}{RT}}$$

Where *D* is the effective diffusion coefficient,

D_0 is the diffusion constant for the fission product in the material ($T \rightarrow \infty$)

Q is the activation energy of diffusion

R is the universal gas constant

T is the absolute temperature

To take into account temperature dependence where different curves are needed for different temperature regions two Arhennius diffusion coefficients can be combined to give:

$$D = D_1 e^{-\frac{Q_1}{RT}} + D_2 e^{-\frac{Q_2}{RT}}$$

Burnup dependence may be taken into account by the following equation:

$$D_0 = C_1[1 + (1+n)C_2 F^n]$$

Where C_1, is C_2 and n are derived from experiments and F the burnup, expressed in FIMA.

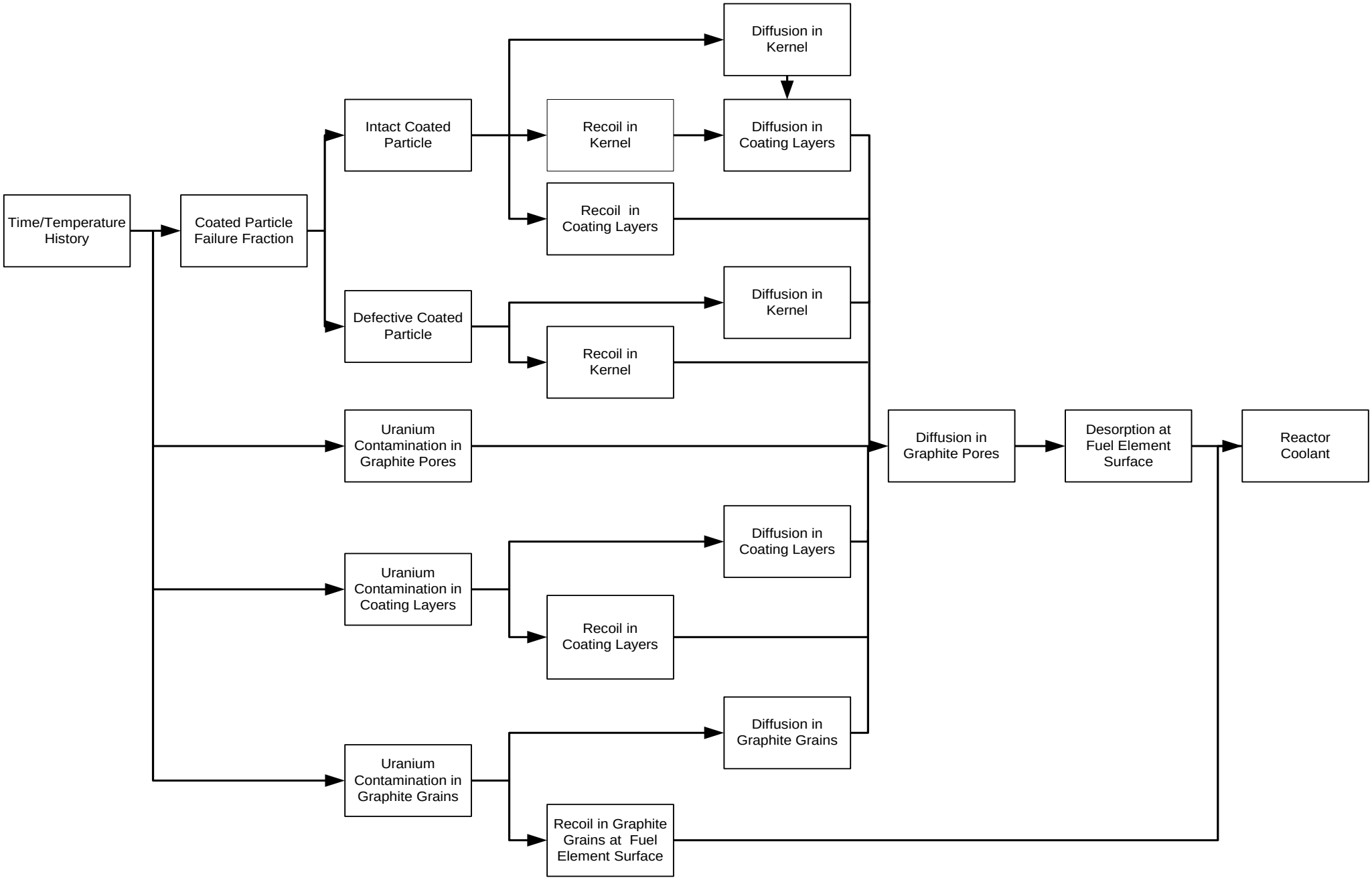

Figure 2: Fission Product Transport Diagram (IAEA, 2010).

2.5 *Past Experiments*

2.5.1 HFR-K3

The irradiation part of the HFR-K3 experiment (Baldwin & Kania, 1990) was performed at the High Flux Reactor (HFR) located at Petten in the Netherlands (IAEA, 2009). The heatup took place at the KÜFA facility in Karlsruhe (Toscano et al., 2004). Four spheres were irradiated for 359 full-power days. Sphere HFR-K3/1 was irradiated in the upper compartment at an operating temperature ranging from 1020°C to 1200°C with a fast neutron fluence of approximately 4.0×10^{25} m^{-2} and burnup of 7.5 % whilst sphere HFR-K3/3 was irradiated in the central compartment at an operating temperature ranging from 700°C to 920°C and fast neutron fluence of approximately 5.9×10^{25} m^{-2} with burnup of 10.6%.

2.5.2 HFR-K6

HFR-K6 spheres were also irradiated in the HFR reactor in Petten and heatup tests performed at the KÜFA facility. The purpose of the irradiation test was to simulate as closely as possible the operating conditions of the HTR Modul (Charollais F;2006). The neutron fluence was approximately 5×10^{25} m^{-2} with a burnup of 9.7% FIMA. The fuel spheres in HFR-K6 were irradiated for 633.6 full-power days in 26 irradiation cycles. For one third of the irradiation time the fuel element centre temperatures were maintained at 800°C and for the other two thirds at 1000°C (Nabieliek, 1993).

2.5.3 HFR-P4

According to (Schenk, 1994) the HFR-P4 experiment was designed to test the performance limits of the LEU TRISO particle during irradiation. In order to determine the number of damaged particles, fission gas releases in the reactor were measured and post-irradiation examinations performed. Only one out of 78,400 particles was found to be defective after irradiation in spite of burnup, fast neutron fluence and irradiation temperatures exceeding predicted HTR-MODUL values. In this instance, the damage probably occurred before irradiation, at the end of pre-activation treatment. No particle defects were observed to have occurred during the heatup phase of the experiment which was representative of a MODUL depressurisation accident.

2.5.4 HRB-22

The objectives of the HRB-22 irradiation and the heatup test (Kazuhiro &Tsutomu, 2003) were to obtain irradiation performance data of the advanced fuel and fuel performance data during accident conditions (Minato et al., 1998). Irradiation of HRB-22 spheres was performed in the High Flux Isotope Reactor at the Oak Ridge National Laboratory for 88.8

full-power days. The maximum burnup and fast neutron fluence was 6.7% FIMA and 2.8 $x10^{25}$ m^{-2} respectively. Temperatures were kept below 1200°C.

2.5.5 HFR-EU1bis

The objective of the HFR-EU1bis test, as stated in Futterera et al. (2008), was to irradiate five HTR fuel pebbles at conditions beyond the characteristics of current HTR reactor designs with pebble bed cores, e.g. HTR-Modul, HTR-10 and PMBR. This was to demonstrate the integrity of the fuel under conditions of increased power conversion efficiency and high fuel centre temperatures of 1250^{o}C compared to 1000–1200^{o}C in earlier tests and an end state burnup close to 16% FIMA, double the license limit of the HTR-Modul.

2.5.6 HTR-PM

The HTR-PM test is a code-to-code comparison exercise with an invented irradiation history (Verfondern, In Press) and not related to the Chinese HTR-PM design. Fuel sphere data is taken from German reference fuel.

3. GETTER Code

3.1 *GETTER Fission Product Release Model*

GETTER (Rollig, 2001) was originally developed and used by the German utility consortium HRB (Hochtemperatur Reaktorbau) during the German HTR programme and subsequently acquired by Westinghouse Reaktor GmbH until its transfer to PBMR in 2001.

The GETTER code is used for long-lived metallic and iodine-131 release calculations for both normal and accident conditions. Using as input, neutron cross-sections and gas temperatures, GETTER calculates fuel burnup, fuel temperatures, fission and activation product inventories during the irradiation phase as well as transport and release from a single fuel sphere in the heatup phase using Fick's law of diffusion (Keshaw and van der Merwe, 2006). Diffusion coefficents and activation energies as input to the GETTER code can be found in (Verfondern, 1997). The verification and validation of the GETTER software is described in the literature (van der Merwe, 2004).

The input data to GETTER includes (Keshaw and van der Merwe, 2006):

- Reactor core geometry (flow channels and core regions).
- CFD analysis output (core geometry and dimensions, helium pressure, flow speeds and circulation times through the core and Main Power System (MPS)).
- VSOP analysis output (fuel residence times, coolant and fuel surface temperatures, fast and thermal neutron fluxes and cross sections).

- Cross sections derived from MCNP analyses.
- Material data (fuel sphere data: uranium loading, enrichment, dimensions, particle failure fraction, uranium contamination; transport data for all fuel materials).
- Fission product yields (^{235}U, ^{239}Pu and ^{241}Pu).
- Reactor-specific data (thermal power, number of fuel spheres, etc.).

The output data from GETTER includes:

- Calculated fuel temperatures.
- Fission powers from U and Pu, as well as burnup.
- Radionuclide inventories in different fuel components.
- The release rates from different fuel components.
- Single sphere weighted core average release.

4. CRP-6 Input Description

A detailed description of the benchmark input parameters for core heatup accident conditions, taken from (Verforndern, In Press) is provided here:

4.1 *Fuel Parameters*

Table 2: Fuel properties

Parameters	Sensitivity Study	Conducted Heating Tests				Planned Heating Tests	
		HFR-P4	HRB-22	HFR-K3	HFR-K6	HFR-EU1bis	HTR-PM
No of cases for benchmark	15	2	2	2	1	1	1
Fuel	Particle	Small sphere	Compact	Sphere	Sphere	Sphere	Sphere
Fuel element type	-	LEU phase 1	91 OPB-7	GLE-3 LEU phase 1	GLE-4 (AVR 21)	GLE-4-2 (AVR 21-2)	HTR-PM
Matrix graphite grade	-	A3-27		A3-27	A3-3	A3-3	A3-3
Matrix density [kg/m^3]	-		1690	1750	1750	1750	1730
Total FE dimension [mm]	-	32 length 23-29 dia	39.0 length 26.0 outer dia 10.0 inner dia	59.98 dia	60 dia	60 dia	60 dia
Fuel zone diameter [mm]	-	20 dia	-	47 dia	50 dia	50 dia	50 dia
No of cp per sphere/compact	-	1631	2800	16,350	14,580	9560	11,240

Packing fraction [%]	-	14.6	6.8 (fuel) 17.1 (dummy)			6.2	7.0
Heavy metal loading [g/FE]	-	1.018	2.323	10.22	9.4346	6.0	7.0
U-235 content [g/FE]	$1.0*10^{-4}$	0.10016	0.095	1.004	1.0	1.005	0.62
Fraction of free uranium	0.		$4.2*10^{-7}$	$3.5*10^{-5}$	0.	$7.8*10^{-6}$	$6*10^{-5}$

Table 3: TRISO particle properties

Parameters	Sensitivity Study	Conducted Heating Tests				Planned Heating Tests	
		HFR-P4	HRB-22	HFR-K3	HFR-K6	HFR-EU1bis	HTR-PM
Coated particle batch		EUO 2308		EUO 2308	EUO 2358-2365	HT 384-393	
Kernel composition	UO_2	LEU UO_2	LEU UO_2	LEU UO_2	LEU UO_2	LEU UO_2	LEU UO_2
Enrichment [U-235 wt.%]	8.0	9.82	4.07	9.82	10.6	16.76	8.9
Kernel diameter [µm]	500	497 ± 14.1	544 ± 9.1	497 ± 14.1	508 ± 10.0	501 ± 10.8	500
Buffer layer thickness [µm]	100	94 ± 10.3	97 ± 12.9	94 ± 10.3	102 ±11.5	92 ±14.3	95
lPyC layer thickness [µm]	40	41 ± 4.0	33 ± 3.4	41 ± 4.0	39 ±3.9	38 ±3.4	40
SiC layer thickness [µm]	35	36 ± 1.7	34 ± 1.6	36 ± 1.7	36 ± 3.4	33 ± 1.9	35
OpyC layer thickness [µm]	40	40 ±2.2	39 ± 3.1	40 ±2.2	38 ± 3.5	41 ± 3.8	40
Kernel density [g/cm^3]	10.81	10.81	10.84	10.81	10.72	10.85	≥10.4
Buffer density [g/cm^3]	1.00	1.00	1.10	1.00	1.02	1.01	≤1.10
lPyC density [g/cm^3]	1.9	~ 1.9	1.85	~ 1.9	1.92 ± 0.005	~ 1.9	1.90
SiC density [g/cm^3]	3.20	3.20	3.20	3.20	3.20	3.20	≥3.18
OPyC density [g/cm^3]	1.88	1.88	1.85	1.88	1.92	1.88	1.90
lPyC Anisotropy BAF	1.053	1.053	1.00		1.08	1.029	≤1.10

OPyC Anisotropy BAF	1.019	1.019	1.00			1.020	≤1.10
Fraction of defective SiC	0	$< 1*10^{-6}$ no defect obs. during irrad.	$3.4*10^{-7}$	$4*10^{-5}$	$1.3*10^{-5}$		$\leq 6*10^{-5}$

4.2 *Sensitivity Study Cases*

All 15 cases selected for the sensitivity study and the associate irradiation and heating conditions are listed in

Table 4.

Cases 1a and 1b refer to caesium release from a bare fuel kernel at two different temperatures. The same heating conditions are used in Cases 2a and 2b for a particle with a kernel, buffer and PyC layer.

Cases 3-5 consider a whole TRISO-coated particle.
All of the cases 3a-e consider heating temperatures of 1600°C and 1800°C. Defects are only taken into account for cases 3d and 3e which contain a broken SiC layer and coating failure respectively.

Cases 4a-d expands on cases 3a-c, 3e and includes an irradiation phase of 500 efpd at 1000°C, preceding the heating phase.

Cases 5a, 5b attempt to simulate the multi-pass conditions in a pebble-bed reactor by using 10 temperature cycles.

Table 4: Sensitivity Study Cases

Sensitivity Study Case	Particle Type	Irradiation Phase				Heating Phase			Radio-nuclides to be calculated
		Time [efpd]	Temperature [°C]	Burnup [% FIMA]	Fast neutron Fluence [10^{25}, E>0.1 MeV]	Temperature T [°C]	Ramp Rate to reach T [K/h]	Time at T [h]	
1a	Bare kernel	-	-	-	-	1200	-	200	Cs-137
1b						1600		200	
2a	Kernel + buffer + IPyC	-	-	-	-	1200	-	200	Cs-137
2b						1600		200	
3a	TRISO coated particle	-	-	-	-	1600	-	200	Cs-137
3b						1800	-	200	
3c						1600 + 1800	Step	200 + 200	
3d	As 3a-c, crack in SiC @ 1800°C					1600 + 1800	Step	200 + 200	Cs-137
3e	As 3a-c, crack in SiC @ 1600°C,					1600 + 1800	Step	200 + 200	Cs-137 Kr-85

Sensitivity Study Case	Particle Type	Irradiation Phase				Heating Phase			Radio-nuclides to be calculated
		Time [efpd]	Temperature [°C]	Burnup [% FIMA]	Fast neutron Fluence [10^{25}, E>0.1 MeV]	Temperature T [°C]	Ramp Rate to reach T [K/h]	Time at T [h]	
	crack in lPyC and OPyC @ 1800°C								
4a	TRISO coated particle	500	1000	10	2	1600	-	200	Cs-137 Ag-110m
4b						1800	-	200	
4c						1600 + 1800	Step	200 + 200	
4d	As 4a-c, crack in SiC @ 1600°C, crack in lPyC and OPyC @ 1800°C					1600 + 1800	Step	200 + 200	Cs-137 Kr-85
5a		10 cycles of	600 → 1000	10	2	-	-	-	Cs-137

Sensitivity Study Case	Particle Type	Irradiation Phase				Heating Phase			Radio-nuclides to be calculated
		Time [efpd]	Temperature [°C]	Burnup [% FIMA]	Fast neutron Fluence [10^{25}, E>0.1 MeV]	Temperature T [°C]	Ramp Rate to reach T [K/h]	Time at T [h]	
5b		100 each				1600	Step	200	Ag-110m

4.3 *Past Experiments*

For the past experiments, a total of seven heatup experiments with fuel samples from four irradiation experiments have been used as part of the postcalculation part of the accident benchmark study, as described in Table 5. The heating temperature vs time history in the heatup phase was fitted to step functions. Failures of coated particles as a function of time were extrapolated from the krypton release records.

The irradiation the HFR-P4 test was conducted to test the limits of the HTR-Modul fuel. Spherical fuel elements had a spherical fuel zone of reduced diameter. No particle failure was observed during irradiation. The two spheres, HFR-P4/1-12 and HFR-P4//3-7, were subjected to burnups of 11.1 and 13.9% FIMA and fast neutron fluences of 5.5 and 7.5×10^{25} m^{-2} (E>0.1 MeV) respectively during the irradiation phase. The heatup phase included temperatures of 1600°C for over 300 hours. HFR-P4/1-12 showed no signs of particle failure whilst particle failures were observed in HFR-P4//3-7 as described in Table 9.

The HRB-22 fuel was in the form of fuel compacts as opposed to spheres which were irradiated up to 7% FIMA with a fast neutron fluence of approximately 2.0×10^{25} m^{-2}. Only three codes postcalculated these two heating tests. The geometry falls outside GETTER's capability and this test was therefore not modelled with GETTER.

The HFR-K3/1 sphere experienced an irradiation phase of 7.5% FIMA burnup and a fast neutron fluence of 4.0×10^{25} m^{-2} (E>0.1 MeV) followed by heatup at 1600°C for over 500 hours. No particle failures were observed. The HFR-K3/3 sphere was irrigated in the same rig with a fluence of $5.9x10^{25}$ m^{-2} (E>0.1 MeV) with burnup of 10.6% and then heated at 1800°C for over 100h. At 25 hours the test was accidentally interrupted and then resumed. Ten hours into heatup at 1800°C particle failures began to occur as described in Table 9.

The irradiation experiment HFR-K6 was designed to test HTR-Modul fuel in order to observe the performance of the fuel under normal operational and accident conditions. The heatup test was only conducted 13 years after irradiation. Sphere 3 had a corrected burnup of 9.7% FIMA and was exposed to a fast neutron fluence of 4.8×10^{25} m^{-2} (E>0.1 MeV). The heatup intervals were 1600, 1700, and 1800°C over periods of 100h each and 1800°C for 300h. Particle failures occurred during the final 1800°C phase as described in Table 9.

Table 5: Past Experiment Cases

Case	Irradiation Phase				Heating Phase		
	Time [efpd]	**Temperature [°C]**	**Burnup [% FIMA]**	**Fast neutron Fluence [10^{25}, E>0.1 MeV]**	**Temperature T [°C]**	**Time to reach T [h]**	**Time at T [h]**
Postcalculation of Heating Tests							
6a HFR-P4-1-12	351 (8424 h)	940	11.1	5.5	300 1050 1250 1600	- 1.5 0.5 7.5	0.5 5.5 13.5 304 Total: 333
6b HFR-P4-3-7	351 (8424 h)	1075	13.9	7.5	300 1050 1250 1600	- 1.5 0.5 7.5	0.5 5.5 13.5 304 Total: 333
7a HRB-22	88.9 (2134 h)	1103 (time av max)	4.8	2.1	20 1650	- 5.4	0.8 -

Case	Irradiation Phase				Heating Phase		
	Time [efpd]	**Temperature [°C]**	**Burnup [% FIMA]**	**Fast neutron Fluence [10^{25}, E>0.1 MeV]**	**Temperature T [°C]**	**Time to reach T [h]**	**Time at T [h]**
Test 3		1031 (time/vol av)			1700	0.8	270 Total: 277
7b HRB-22 Test 4	88.9 (2134 h)	1103 (time av max) 1031 (time/vol av)	4.8	2.1	20 1750 1800	- 5.8 0.8	0.4 - 222 Total: 229
8a HFR-K3/1	359 (8616 h)	1020(s)-1216(c)	7.5	4.0	300 1050 1250 1550 300 1600	- 1.5 0.5 6.5 1 9	0.5 5.5 16.5 - - 500 Total: 541
8b HFR-K3/3	359 (8616 h)	700(s)-983(c)	10.6	5.9	300 1050 1250	- 1.5 0.5	0.5 5.5 13.5

Case	Irradiation Phase				Heating Phase		
	Time [efpd]	**Temperature [°C]**	**Burnup [% FIMA]**	**Fast neutron Fluence [10^{25}, E>0.1 MeV]**	**Temperature T [°C]**	**Time to reach T [h]**	**Time at T [h]**
					1800	12	25.5
					300	1	-
					1050	1.5	19.5
					1250	0.5	19
					1800	12	74.5
							Total: 187
9	634	1140 (s)	10.9	4.8	300	-	7
HFR-K6/3	(15,216 h)				1050	2	13.5
					1600	11	99
					20	17	-
					1700	5.5	100
					20	17	-
					1800	2	100
					20	17	-
					300	7	-
					1800	1	300

Case	Irradiation Phase				Heating Phase		
	Time [efpd]	**Temperature [°C]**	**Burnup [% FIMA]**	**Fast neutron Fluence [10^{25}, E>0.1 MeV]**	**Temperature T [°C]**	**Time to reach T [h]**	**Time at T [h]**
							Total: 699

4.4 *Prediction Tests*

The HFR-EU1 irradiation experiment was focused on testing the performance limits of German and Chinese high-quality fuel at high burnup in line with the European Union's renewed focus on HTGR fuel testing. HFR-EU1bis is a simplified, precursor test at high temperatures. When the CRP-6 benchmark was defined the HFR-EU1bis experiment was still only a prediction test, as neither the irradiation nor heatup phase had been conducted. It had been defined to have an irradiation phase with burnup of 9.3% FIMA and a fast neutron fluence of 3×10^{25} m^{-2} (E>0.1 MeV), and heatup at 1250, 1600, 1700, and 1800°C for 200 hours each. Subsequently, the irradiation and heatup tests have been concluded without the 1800°C heating phase and caesium and silver data published. No particle failure was assumed to have occurred.

As previously mentioned, the "HTR-PM" is a fictitious test for code benchmarking using German reference fuel specifications. No particle failure is assumed to occur during heating.

Table 6: Future Experiment Cases

Case	Irradiation Phase				Heating Phase		
	Time [efpd]	**Temperature [°C]**	**Burnup [% FIMA]**	**Fast neutron Fluence [10^{25}, E>0.1 MeV]**	**Temperature T [°C]**	**Ramp Rate to reach T [K/h]**	**Time at T [h]**
Prediction of Heating Tests							
10 HFR-EU1bis/1	249 (5976 h)	1100 (s)	9.3	3.0	300 1250 1600 1700 1800	- 19 7 2 2	6 200 200 200 200

							Total: 836
11 HTR-PM	1000 (24,000 h)	1000	9	2 ~ 5	300 1250 1600 1650 1700 1800	- 2 7.5 1 1 2	0.5 10 200 200 200 200 Total: 824

Table 7: Diffusion Coefficients for Accident Conditions

	D_1 [m^2/s]	Q_1 [kJ/mol]	D_2 [m^2/s]	Q_2 [kJ/mol]
Caesium				
in UO_2	$5.6*10^{-8}$	209	$5.2*10^{-4}$	362
in buffer	$1*10^{-8}$	0		
in PyC	$6.3*10^{-8}$	222		
in SiC	$5.5*10^{-14} * e^{\Gamma/5}$	125	$1.6*10^{-2}$	514
in matrix A3-3	$3.6*10^{-4}$	189		
in matrix A3-27	$3.6*10^{-3}$	189		
Strontium				
in UO_2	$2.2*10^{-3}$	488		
in buffer	$1*10^{-8}$	0		
in PyC	$2.3*10^{-6}$	197		
in SiC	$1.2*10^{-9}$	205	$1.8*10^{6}$	791
in matrix	$1.0*10^{-2}$	303		
Silver				
in UO_2	$6.7*10^{-9}$	165		
in buffer	$1*10^{-8}$	0		
in PyC	$5.3*10^{-9}$	154		
in SiC	$3.6*10^{-9}$	215		
in irradiated matrix A3-3	1.6	258		
Krypton				

	D_1 [m^2/s]	Q_1 [kJ/mol]	D_2 [m^2/s]	Q_2 [kJ/mol]
(Iodine)				
in UO_2	$8.8*10^{-15}$	54	$6.0*10^{-1}$	480
in buffer	$1*10^{-8}$	0		
in PyC	$1*10^{-30}$	0		
in SiC	$1*10^{-30}$	0		
in matrix	$6.0*10^{-6}$	0		

Table 8: Initial Uranium Distribution

Layer	**U/U_{total}:**
Buffer:	$1*10^{-3}$
IPyC:	$1*10^{-4}$
SiC:	$1*10^{-6}$
OPyC:	$1*10^{-6}$
Matrix:	$1*10^{-6}$

Table 9: Particle Failure During Heatup

Case	Test	Failure Fraction
6a	HFR-P-4-1-12	No
6b	HFR-P-3-7	1st cp after 49 h at 1600°C 2nd cp after 115 h 3rd cp after 200 h
7a	HRB-22-3	No
7b	HRB-22-4	1 cp failed during heat-up at T = 1400°C
8a	HFR-K3/1	No
8b	HFR-K3/3	Gradual increase of Kr release after 10 h heating

		at 1800°C exceeding level of 1 failed cp ($6*10^{-5}$) after 50 h at 1800°C 55 h 65 h 70 h 75 h 80 h 85 h 89 h 92 h 97 h
9	HFR-K6/3	Gradual increase of Kr release with beginning of final heating phase exceeding level of one failed cp ($1*10^{-4}$) after 119 h at 1800°C (final heating phase) 174 h 214 h 258 h 288 h

5. Results

It should be noted that for all results below, the fractional release presented is the fractional release during heating, where the fractional release at the end of irradiation is subtracted from the total fractional release to give the net fractional release during heatup.

It should also be taken into account that GETTER takes only one diffusion coefficient constant and related activation energy as input per radionuclide. In Table 7, two diffusion coefficients are presented for caesium to adequately represent behaviour at low and high temperatures. It is currently not possible to implement two diffusion coefficients for a single radionuclide in GETTER. A combined diffusion coefficient was derived by plotting the individual diffusion coefficients and using a correlation to obtain the combined diffusion coefficient parameter values, D, for temperatures above 1400 C.

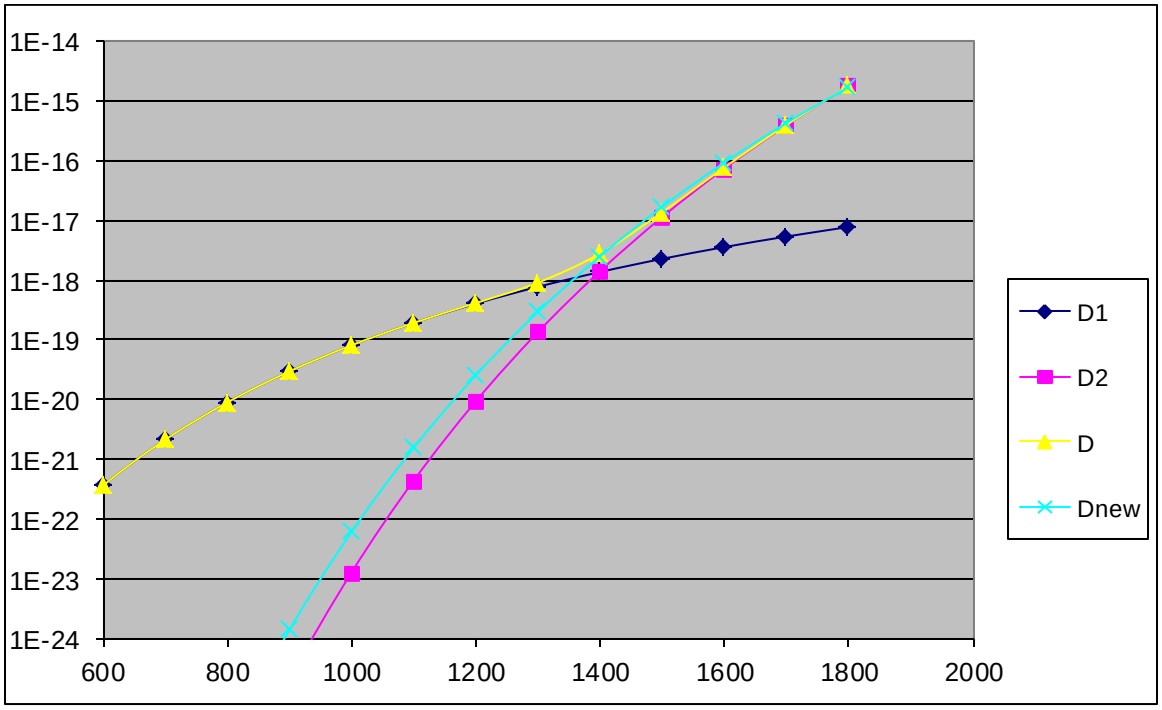

Figure 3: Derived Diffusion Coefficient for Caesium to be used in GETTER

5.1 *Sensitivity Cases 1 -5*

5.1.1 Sensitivity Case 1

This case can also be calculated analytically by applying the fractional release term derived from the Equivalent Sphere model (Nabielek, 1974).

Table 10: Sensitivity Case 1 Results

Participant	Fractional Release of ^{137}Cs from a bare kernel	
	Case 1a (1200°C)	Case 1b (1600°C)
France	0.472	1.000
Germany	0.456	1.000
Korea	0.473	1.000
RSA	**0.498**	**1.000**
US/GA	0.453	0.970
US/INL	0.467	1.000
US/NRC	0.463	0.998
US/SNL	0.465	1.000
Analytical solution	**0.4673**	**0.99999959**

GETTER results are slightly higher than the analytical solutions and the other codes as it requires an irradiation phase to precede a heat-up phase so that transport during the irradiation phase (recoil and knock on effects) influences the release fraction during heat-up causing GETTER to overestimate the release when compared with heat-up diffusion only.

5.1.2 Sensitivity Case 2

Table 11: Sensitivity Case 2 Results

Participant	Fractional Release of ^{137}Cs from a bare kernel + buffer + pyrocarbon layer	
	Case 2a (1200°C)	Case 2b (1600°C)
France	0.028	0.995
Germany	0.026	0.991
Korea	0.029	0.995
RSA	**0.030**	**0.993**
US/GA	0.006	0.968
US/INL	0.026	0.996
US/NRC	0.026	0.989
US/SNL	0.026	0.995

Similar to case 1, GETTER slightly overestimates the release fraction due to irradiation phase transport.

The comparison shows that all codes, except the GA code, have a fractional release of 2.6-3.0% in the 1200°C case and more than 99% for the 1600°C case. The GA code is an outlier with less than 1% for the 1200°C and less than 97% for the 1600°C case.

5.1.3 Sensitivity Case 3

Table 12: Sensitivity Case 3 Results

Participant	Fractional Release from a TRISO-coated particle					
	Case 3a	Case 3b	Case 3c	Case 3d	Case 3e	
	^{137}Cs	^{137}Cs	^{137}Cs	^{137}Cs	^{137}Cs	I, gases
	after 200 h		after 400 h			
France	6.59 (-5)	0.207	0.222	0.999	0.97	0.98
Germany	1.15 (-3)	0.218	0.239	1.000	1.00	1.00
Korea	4.72 (-4)	0.210	0.224	1.000	1.00	1.00
RSA	**1.14 (-4)**	**0.203**	**0.230**	**1.000**	**1.000**	

US/INL	1.32 (-4)	0.208	0.222	1.000	1.00	1.00
US/NRC	1.25 (-4)	0.207	0.22			
US/SNL	1.00 (-4)	0.208				

As part of the definition of Case 3 no irradiation phases are defined but due to the presence of the SiC layer the overestimation seen in the GETTER calculations in Case 1 and 2 is no longer evident due to the high retention properties of the SiC layer. The German results in Case 3a, 3b and 3c are higher than the other codes due to an incorrect diffusion coefficient having been used. Taking this into account it can be seen that there is good agreement amongst the code results.

Cases 3d and 3e involve defective particles heated up at 1600°C and 1800°C for 200 hours each and thus most of the codes predict a full release of the caesium inventory as expected. In 3d the crack in the SiC layer occurs at the start of the 1800°C phase whereas for 3e the crack in the SiC layer occurs at the start of the 1600°C phase followed by cracks in the PyC layers at 1800°C. Due to the fact that the SiC layer accounts for the majority of the retention in the TRISO particle the metallic fission product release is dominated by the failure of the SiC layer and only slightly accelerated by the failure of the PyC layers. The failure of the PyC layers, however, is important for the release of Kr-85 and other fission gases.

5.1.4 Sensitivity Case 4

Table 13: Sensitivity Case 4 Results

Participant	**Fractional Release from an irradiated TRISO coated particle**			
	Case 4a	**Case 4b**	**Case 4c**	**Case 4d**
	after 200 h		**after 400 h**	
^{137}Cs				
France	2.55 (-4)	0.20	0.21	1.00
Germany	1.47 (-3)	0.22	0.24	1.00
Korea	8.25 (-4)	0.21	0.23	1.00
RSA	**1.64 (-4)**	**0.21**	**0.23**	**1.00**
US/INL	4.10 (-4)	0.23	0.23	1.00
^{110m}Ag				

France	0.27	0.58	0.98	0.98
Germany	0.41	0.87	0.92	1.00
Korea	0.55	0.95	0.98	1.00
RSA	**0.42**	**0.88**	**0.93**	**1.00**
US/INL	0.43	0.89	0.93	1.00

Case 4 also treats a complete TRISO particle, but this time includes a preceding irradiation history. Releases are similar to those in Case 3 but perhaps could be considered to be marginally higher which would be due to the diffusion during the irradiation phase for GETTER, as discussed previously.

5.1.5 Sensitivity Case 5

Table 14: Sensitivity Case 5 Results

Participant	**Fractional Release from a cycles-irradiated TRISO coated particle**			
	Case 5a		**Case 5b**	
	^{137}Cs	**^{110m}Ag**	**^{137}Cs**	**^{110m}Ag**
	after irradiation		**after 200 h heating**	
France	3.78 (-12)	1.57 (-5)	6.44 (-4)	0.14
Germany	2.19 (-19)	5.55 (-6)	1.22 (-3)	0.39
Korea	1.92 (-11)	1.25 (-5)	6.63 (-4)	0.54
RSA	**8.22 (-07)**	**1.47 (-5)**	**1.21 (-4)**	**0.41**
US/INL	6.45 (-14)	5.06 (-5)	3.07 (-4)	0.42

The very low fractional release of caesium in Case 5a is explained by the low irradiation temperature. The large variance in results may be to do with numerical effects which dominate at low concentrations and low releases. Silver has larger releases and thus the variance in results is much smaller, approximately an order of magnitude.

5.2 *HFR-P4*

5.2.1 HFR-P4/1-12

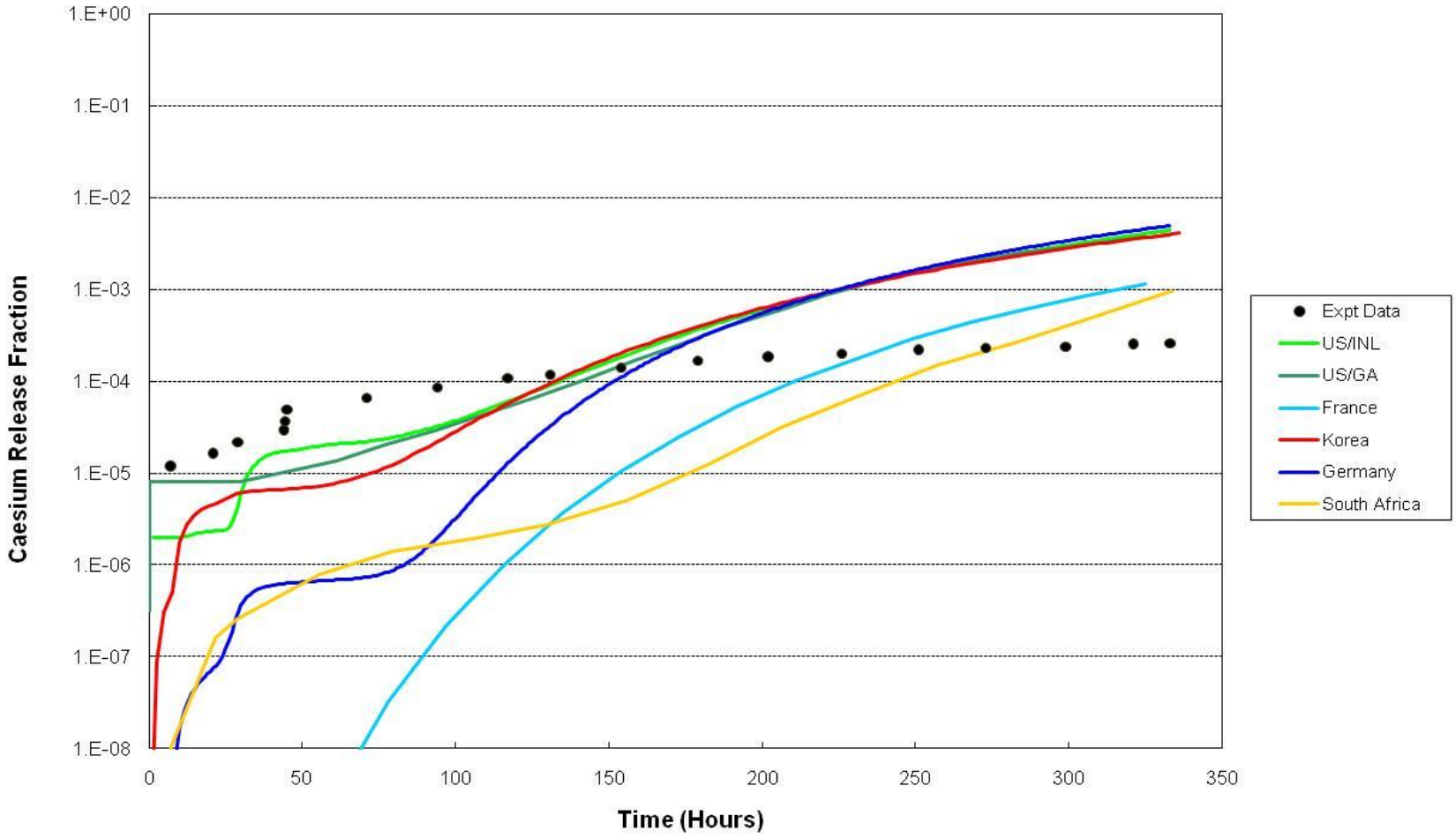

Figure 4: Fractional release of ^{137}Cs from HFR-P4/1-12

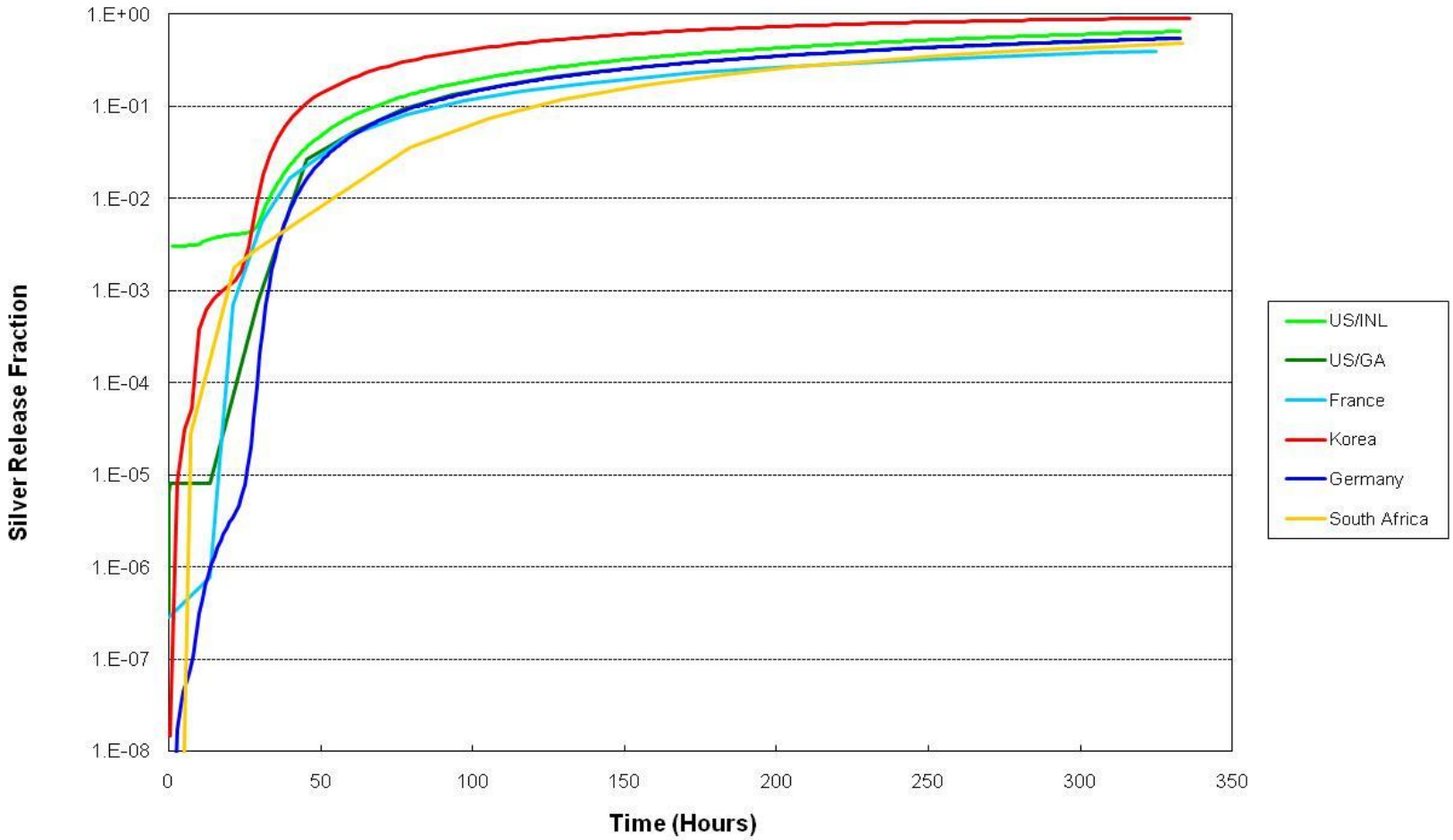

Figure 5: Fractional release of ^{110m}Ag from HFR-P4/1-12.

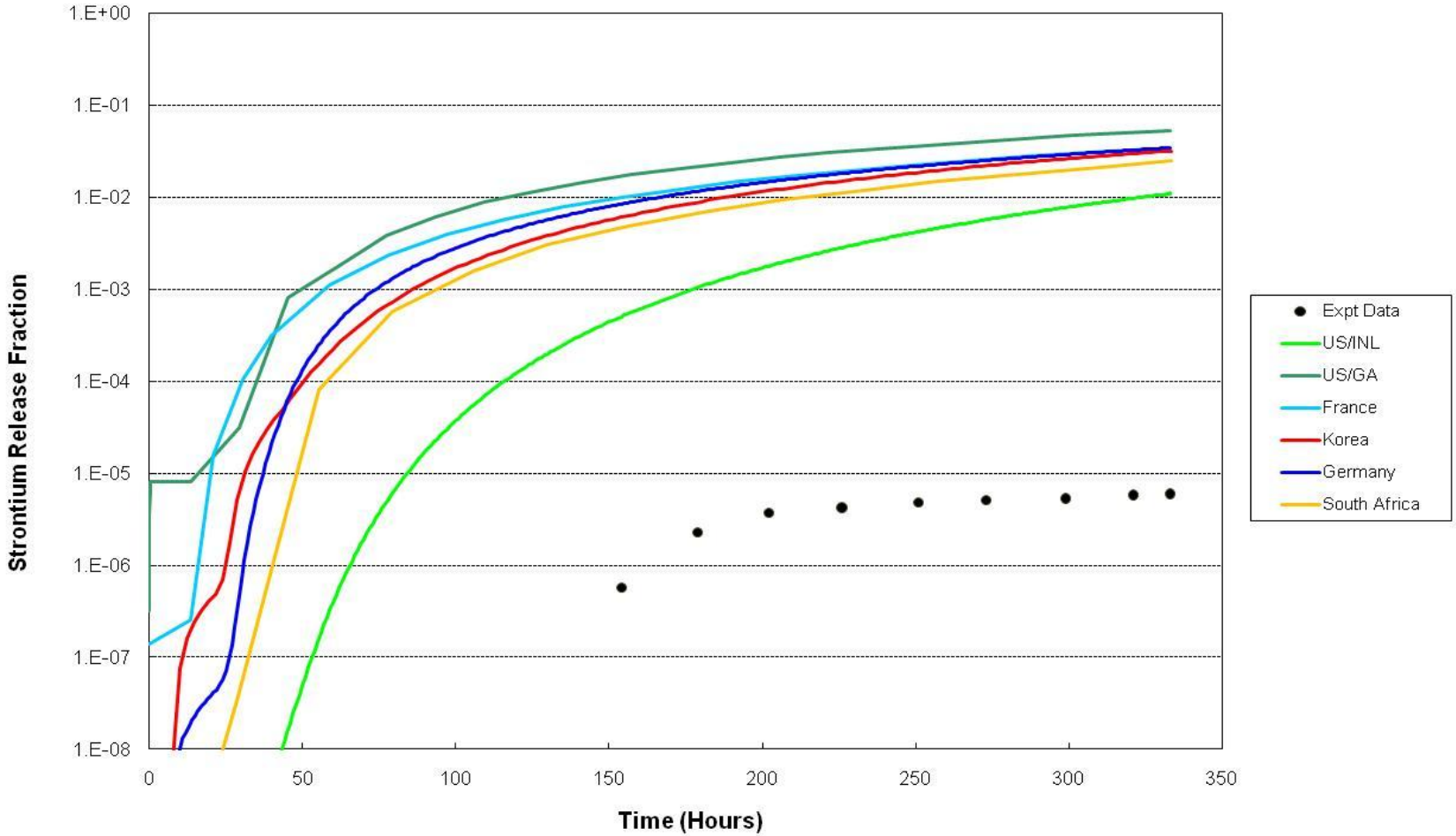

Figure 6: Fractional release of ^{90}Sr from HFR-P4/1-12

As seen in Figure 4 - Figure 6 experimental data is only available for caesium and strontium but not for silver. The high initial release in the caesium curve in Figure 4 suggests a defective TRISO particle. All curves begin below the experimental results but finish higher. The South African and French release fractions are almost an order of magnitude below the other codes. It needs to be taken into account, however, that the compact geometry is not verified or validated in GETTER, and inferior results are to be expected. GETTER results are consistent with the other codes for strontium and silver releases. The variation in the silver release, between codes, is approximately 50% between the lowest and highest values. For both the caesium and strontium curves the difference between codes is greater in the first half of the experiment than in the second half. For strontium, the codes are orders of magnitude higher than the experimental results.

5.2.2 HFR-P4-3-7

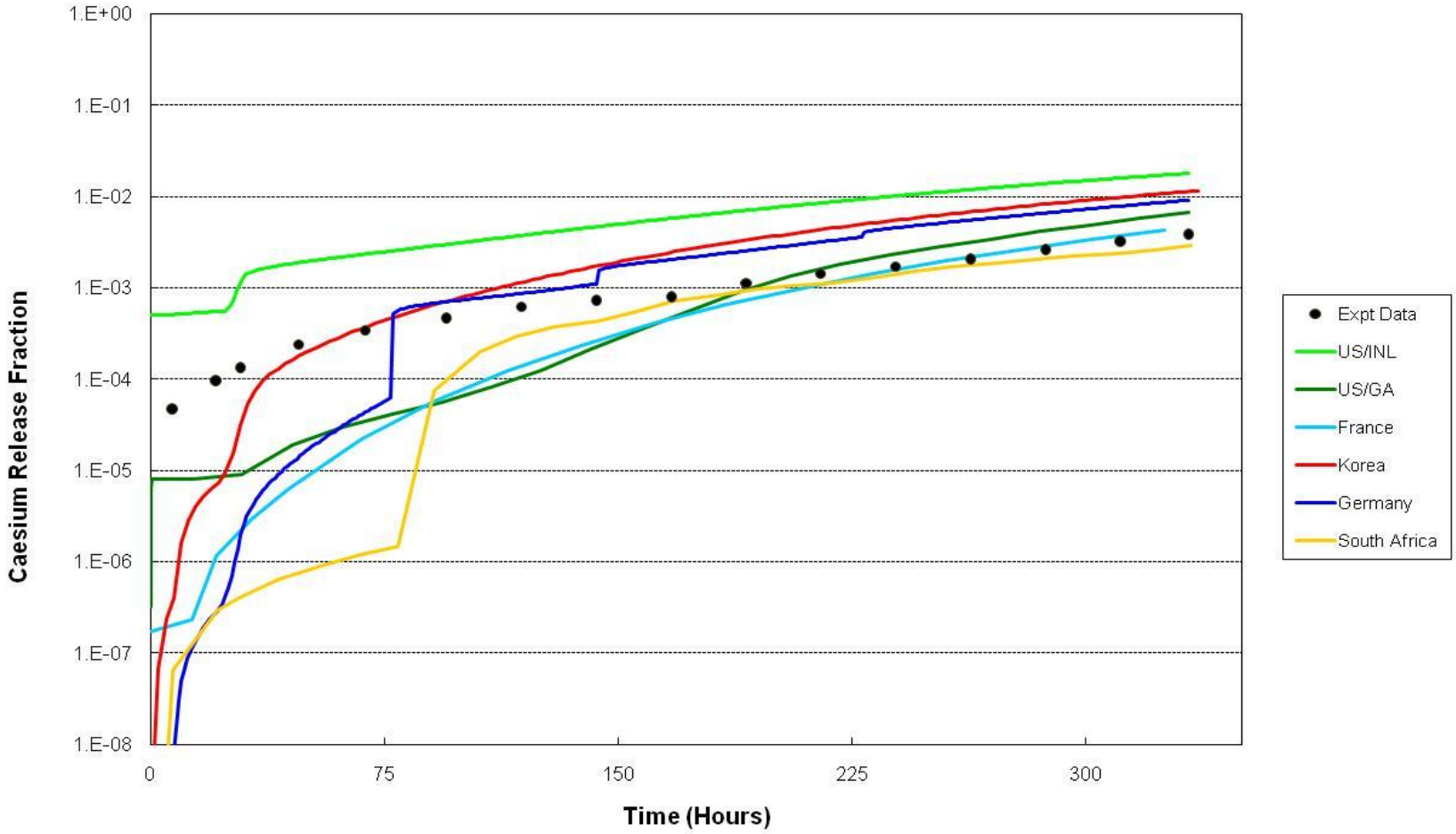

Figure 7: Fractional release of ^{137}Cs from HFR-P4/3-7

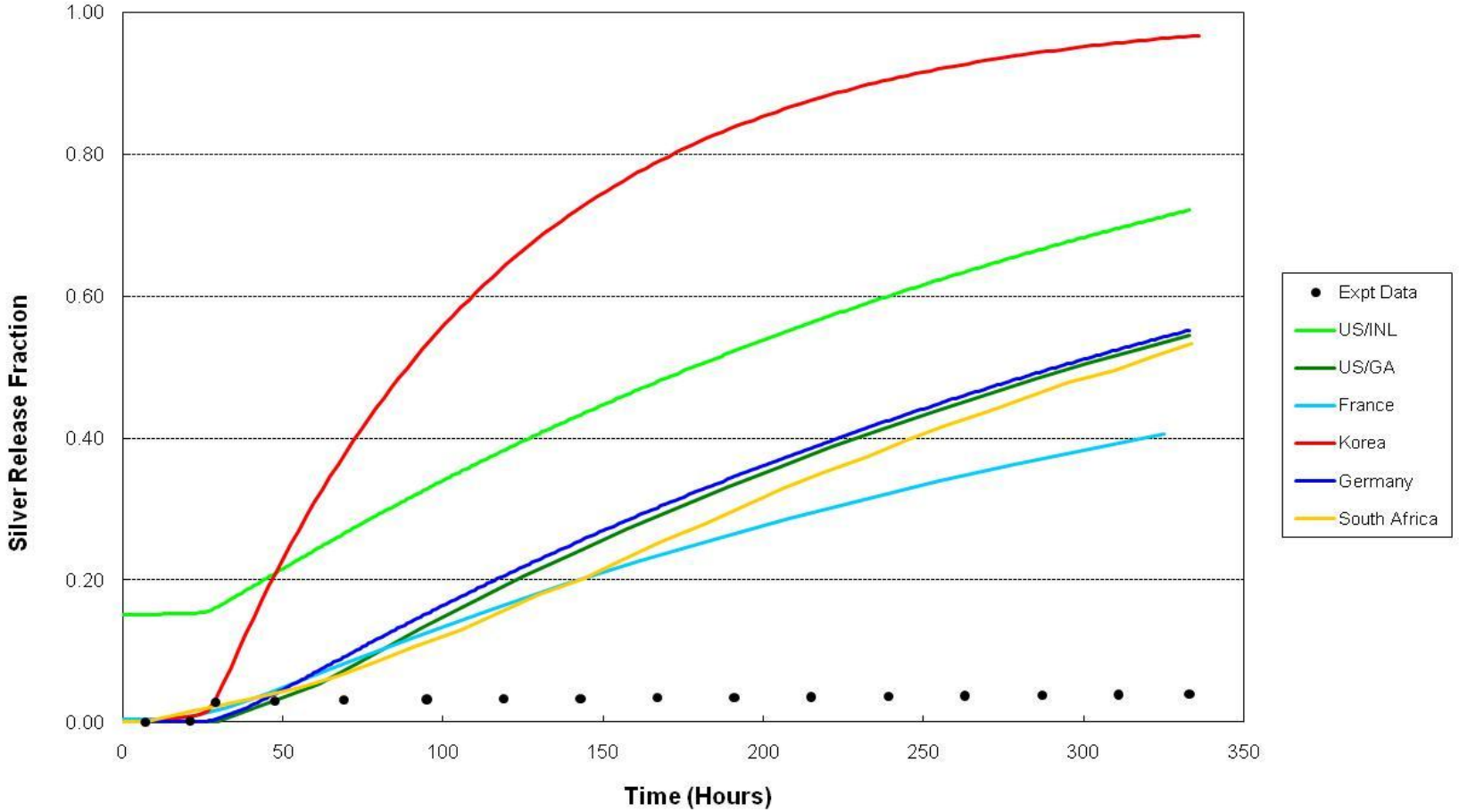

Figure 8: Fractional release of ^{110m}Ag from HFR-P4/3-7

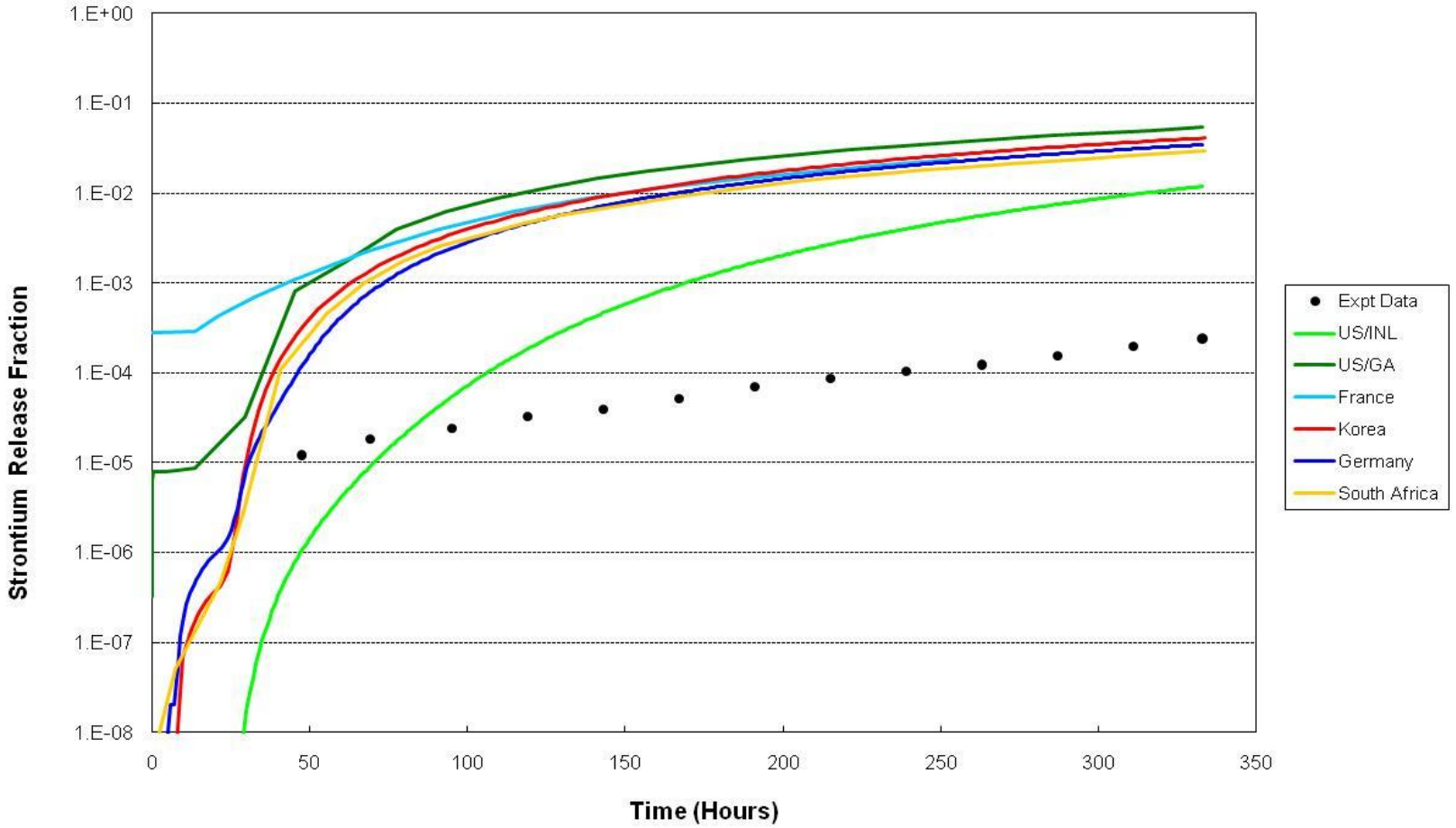

Figure 9: Fractional release of ^{90}Sr from HFR-P4/3-7

Experimental data is available for caesium, strontium, and silver. It is to be noted that fractional releases are higher for HFR-P4/3-7 than for HFR-P4/1-12 due to the combined presence of higher burnup and failed particles in HFR-P4/3-7. Far better agreement with experimental results is observed in Figure 7 for HFR-P4/3-7 than for HFR-P4/3-1. Failures of particles can be explicitly seen in the FRESCO and GETTER curves in the step increase in the fractional release. Codes with a fractional release above the failure fraction would not display a step increase whilst codes with fractional releases below the failure fraction will display a step increase. The steps may therefore not be visible. The ATLAS code appears not to have taken into account the three particle failures. Similar to HFR-P4/1-12 the codes show good agreement between themselves for the caesium and strontium curves but poor agreement for the silver curve. The codes significantly over-predict the experimentally-measured release for strontium and silver. For silver the codes agree with the experimental results until the silver curve flattens which cannot be taken into account by the codes which are based on diffusion theory.

5.3 *HRB-22*

Tests were not performed with GETTER due to issues with the geometry of HRB-22. The fuel for HRB-22 is in compact form and GETTER has not been validated for fuel other than standard pebbles. Thus, to use GETTER for this case would be pushing the code far beyond its range of validation.

5.4 *HFR-K3*

5.4.1 HFR-K3/1

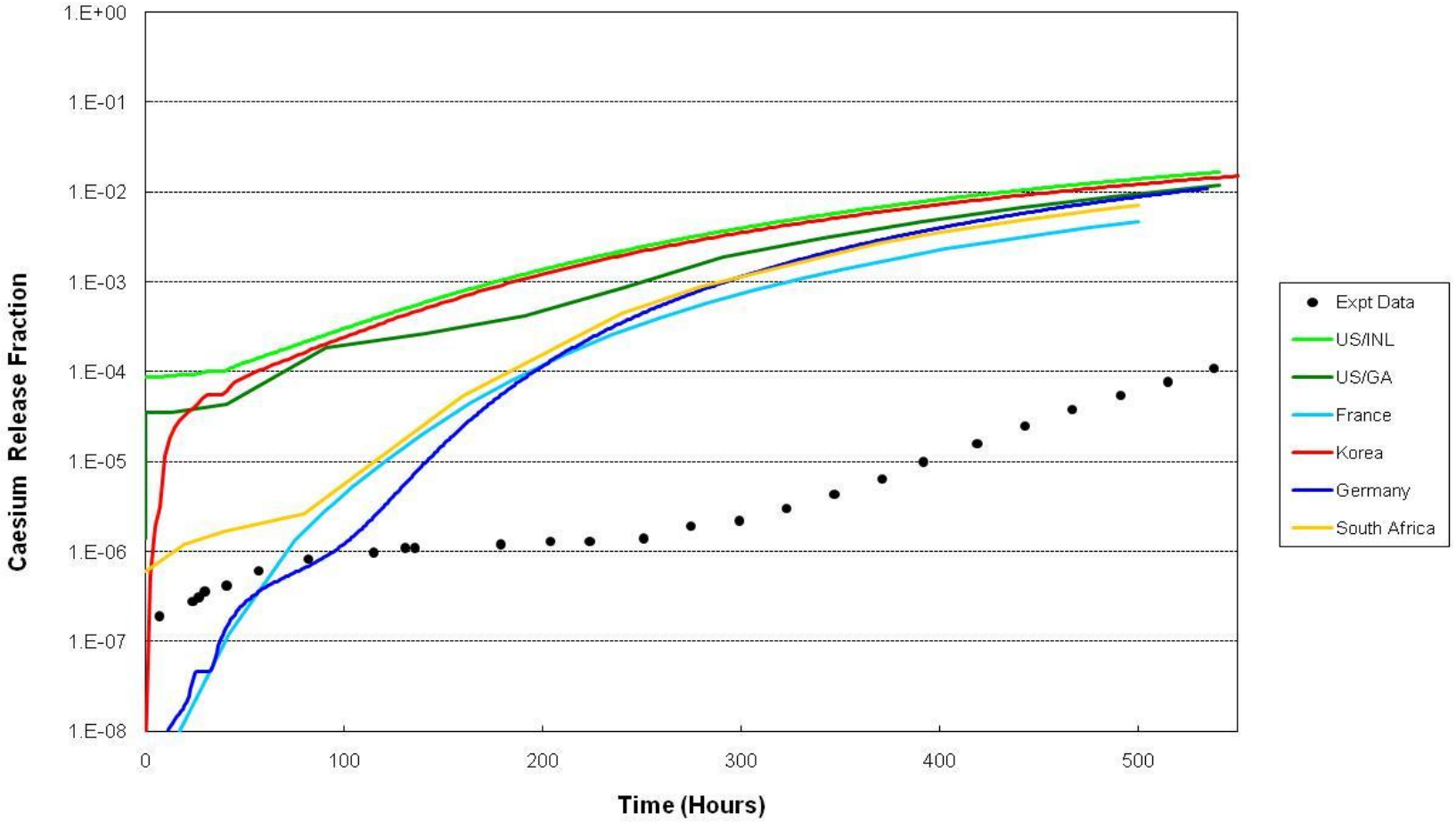

Figure 10: Fractional release of ^{137}Cs from HFR-K3/1

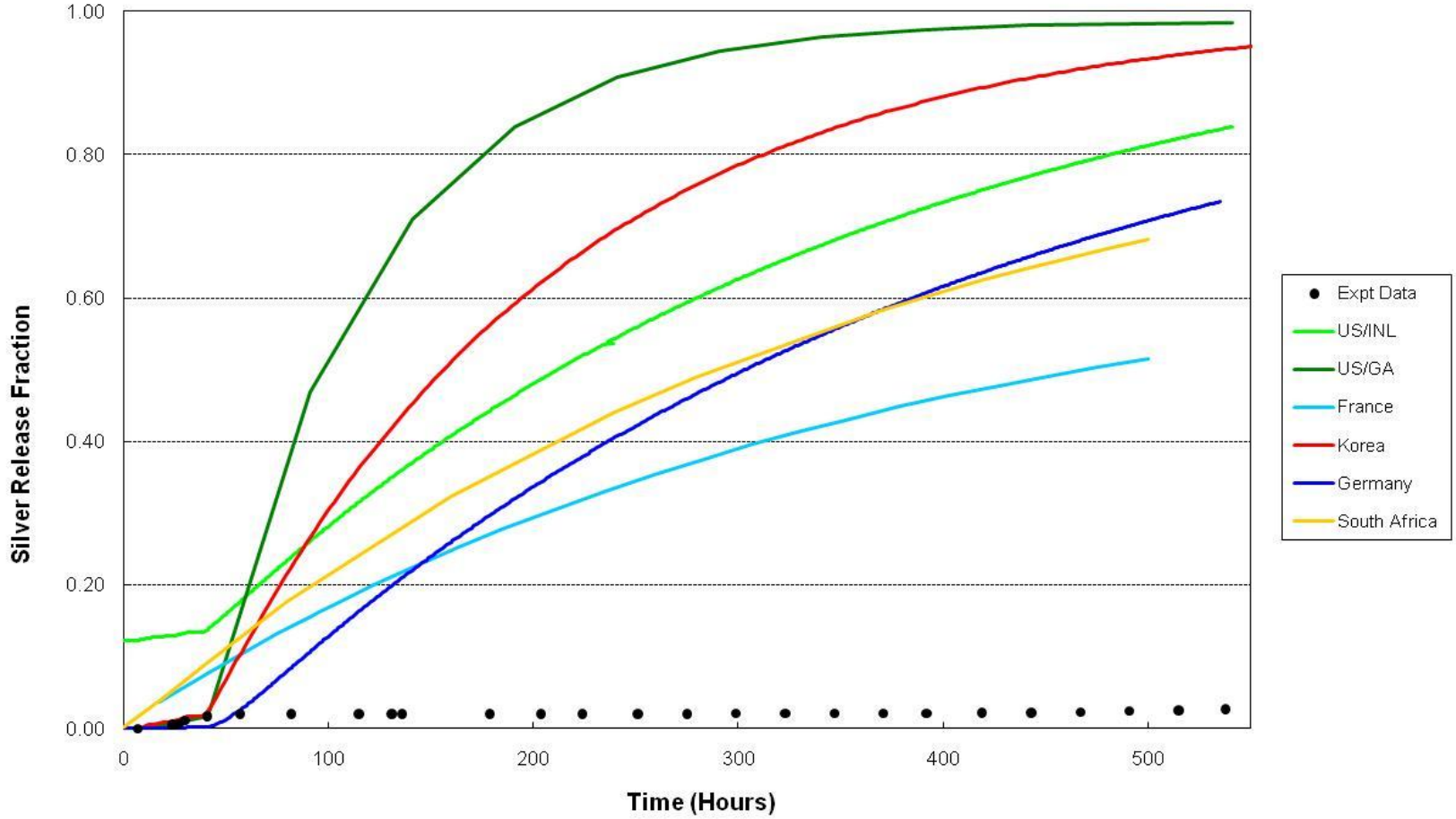

Figure 11: Fractional release of ^{110m}Ag from HFR-K3/1

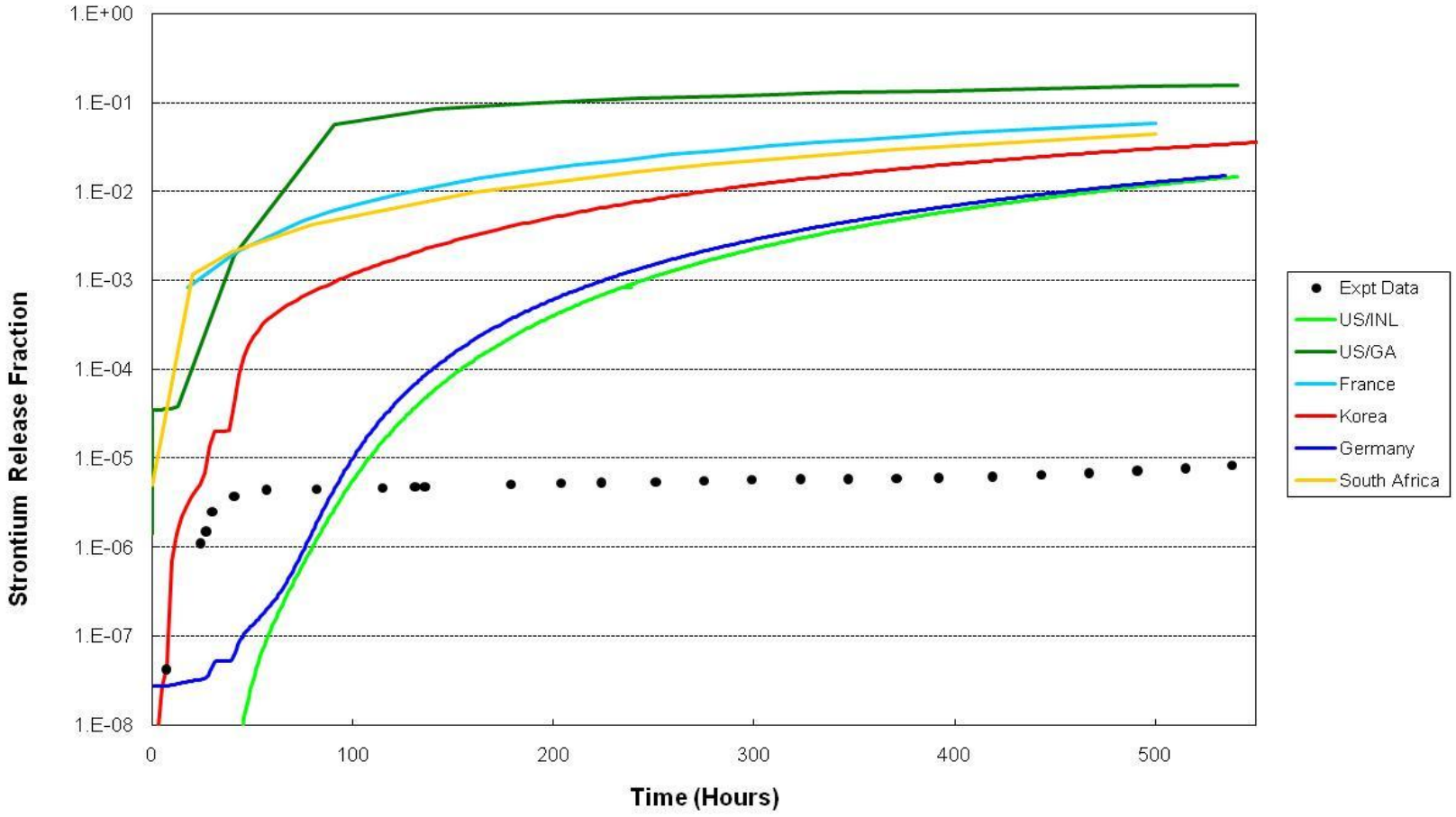

Figure 12: Fractional Release of ^{90}Sr from HFR-K3/1

For all three radionuclides in Figure 10 - Figure 12 it is observed that the experimental results are over-predicted significantly by all codes. The experimental caesium release curve increases initially followed by a plateau and then a further increase whilst for the experimental data curves for both silver and strontium, there is an initial increase followed by the curves flattening out which, as mentioned previously, cannot be modelled by a simple diffusion model.

5.4.2 HFR-K3/3

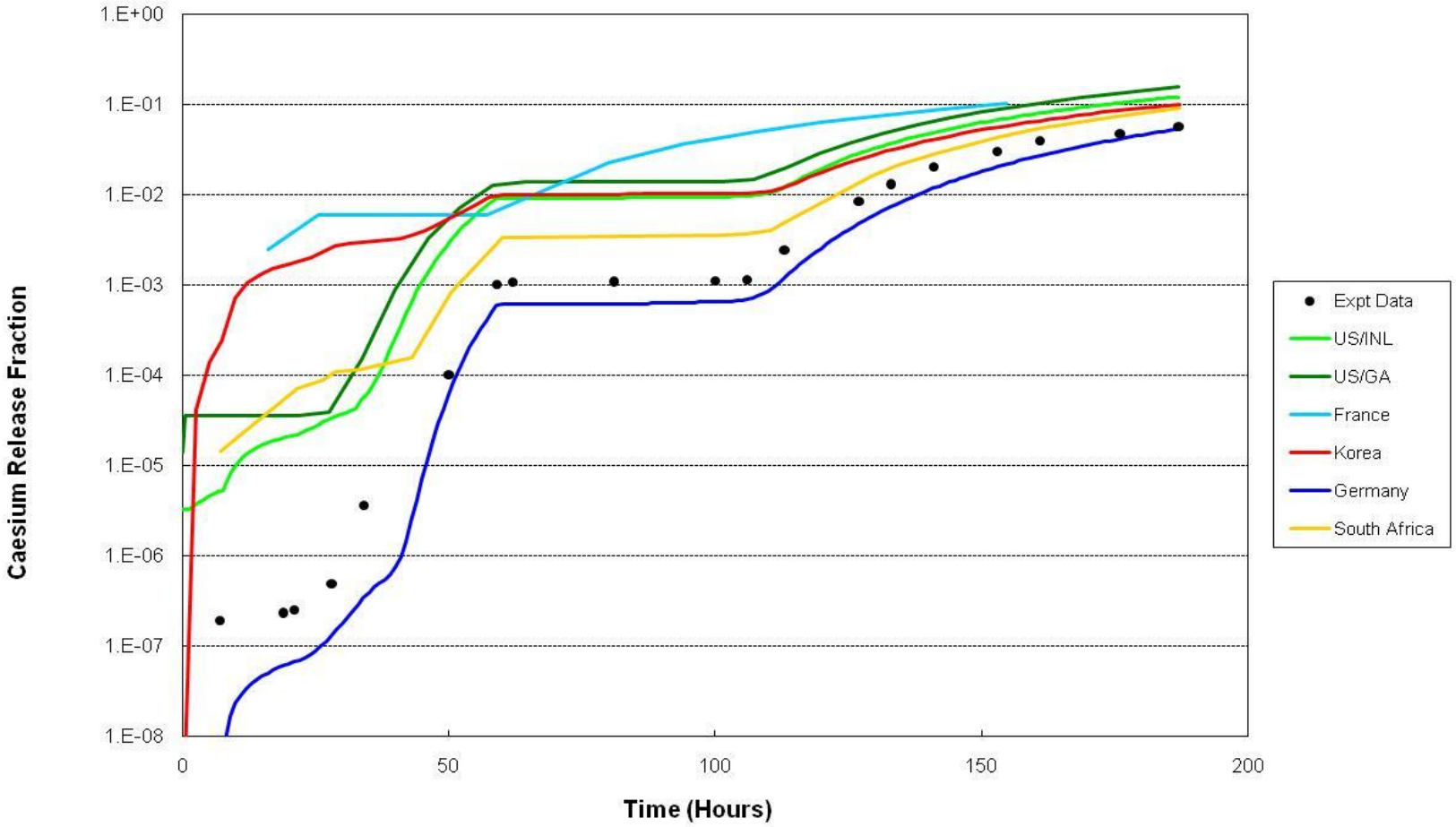

Figure 13: Fractional release of ^{137}Cs from HFR-K3/3

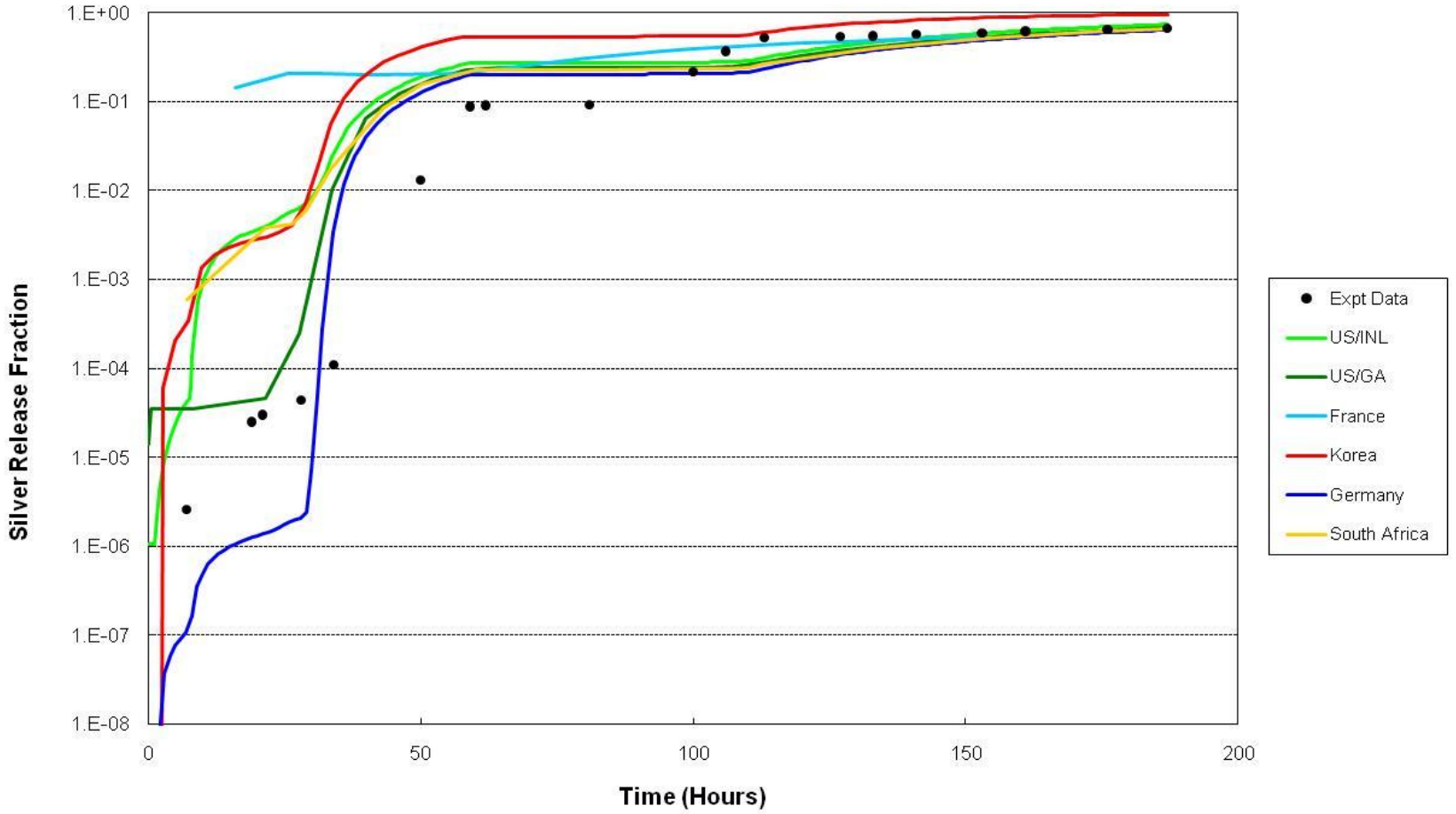

Figure 14: Fractional release of ^{110m}Ag from HFR-K3/3

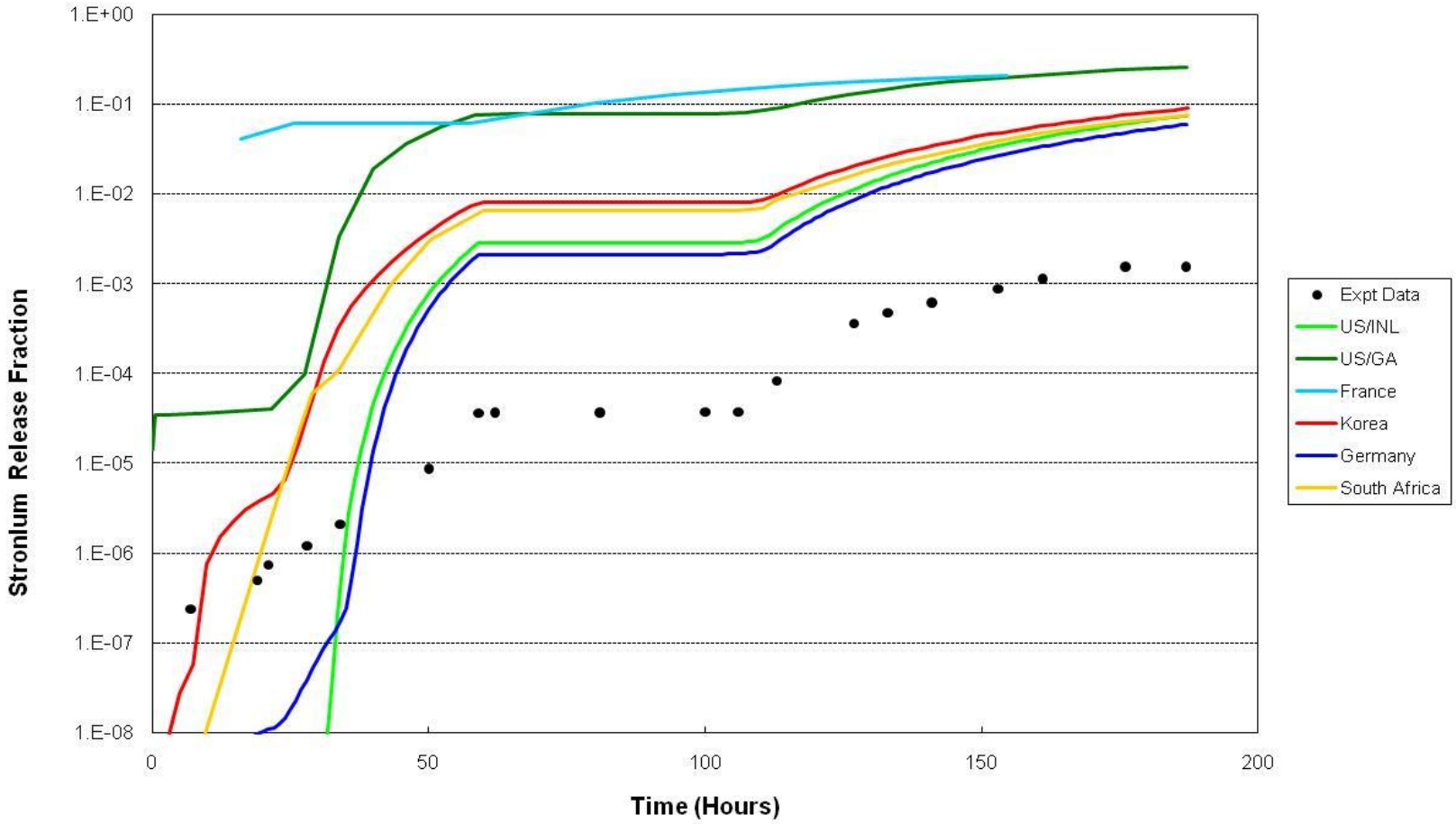

Figure 15: Fractional release of ^{90}Sr from HFR-K3/3

Good agreement is seen between the codes and experimental curves in terms of the evolution of the curves and the actual releases. All curves, even the silver curve, show diffusion like behaviour in contrast to the HFR-P4 and the HFR-K3/1 experiments. For caesium and silver the code results and experimental data are the same order of magnitude whilst for strontium the codes over predict the experimental results by an order of magnitude.

5.5 *HFR-K6*

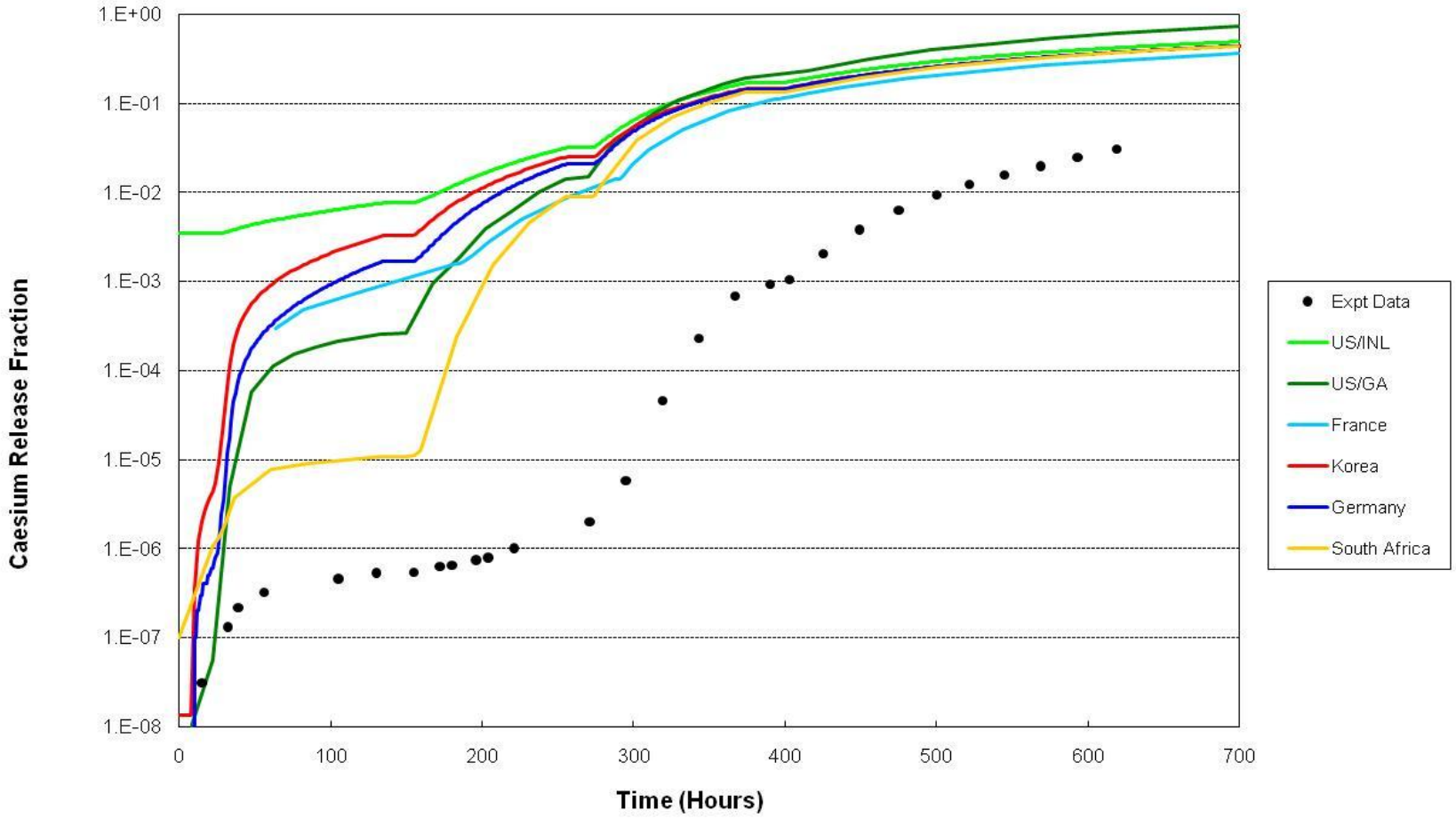

Figure 16: Fractional release of ^{137}Cs from HFR-K6/3

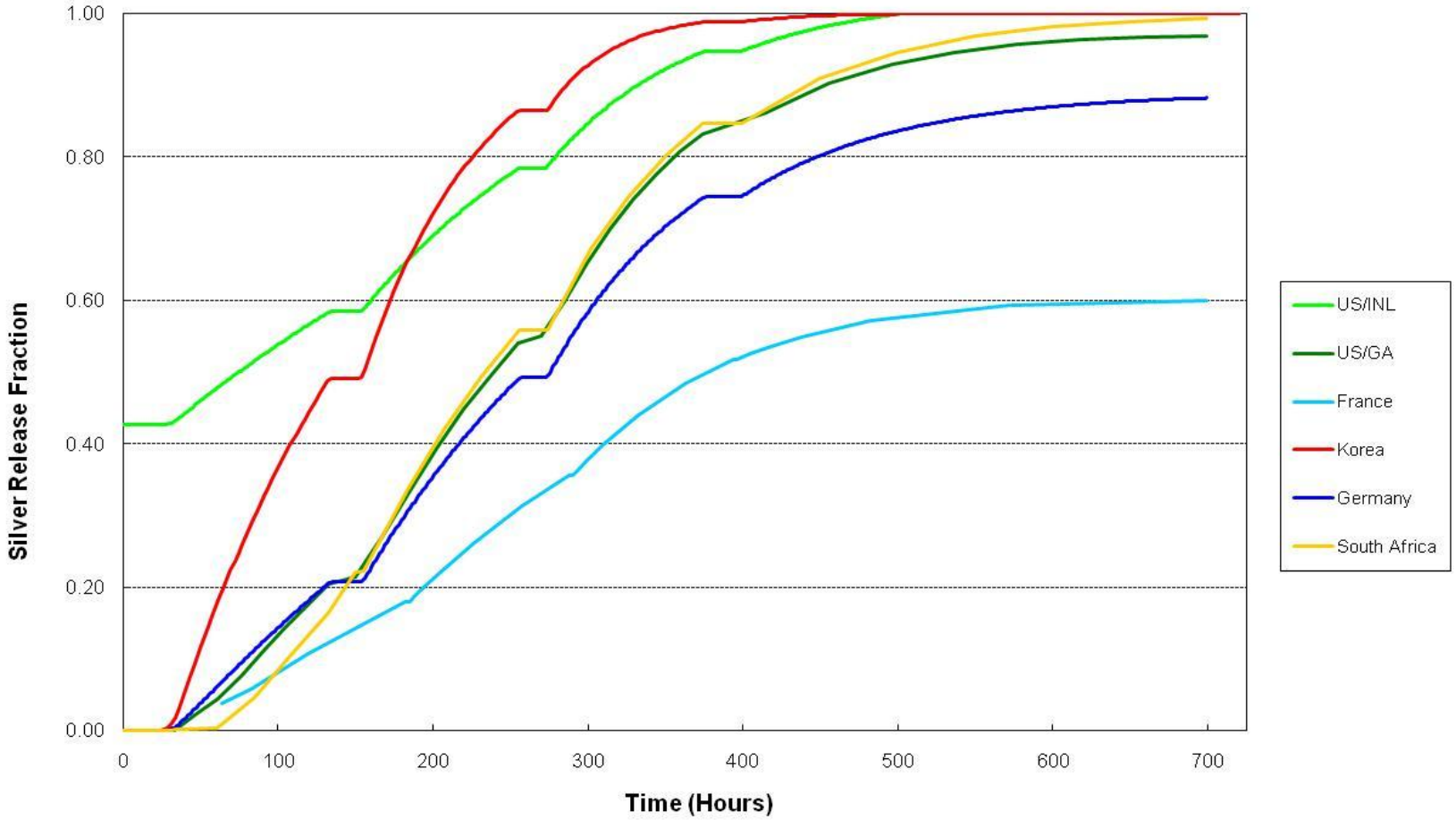

Figure 17: Fractional release of ^{110m}Ag from HFR-K6/3

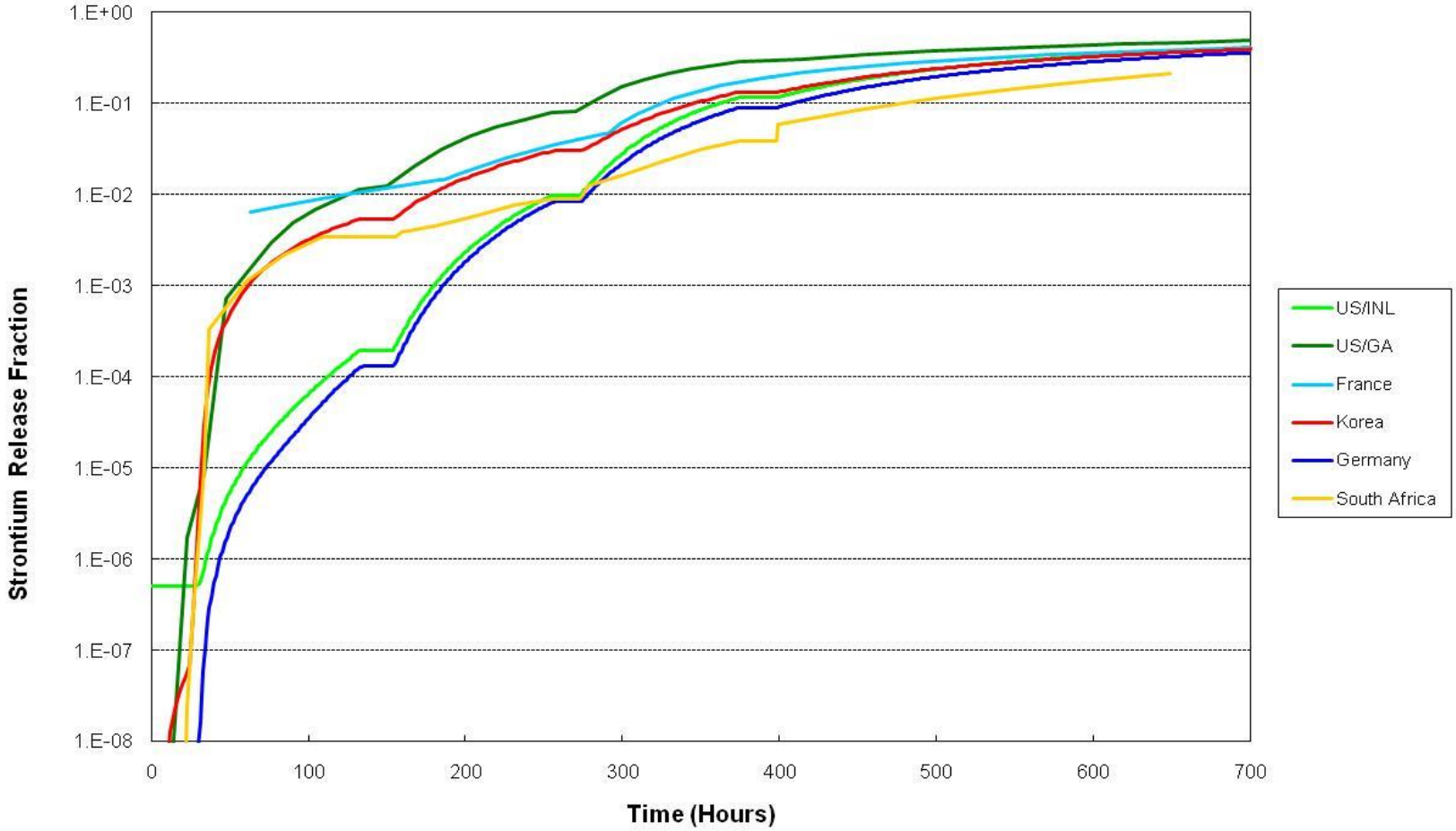

Figure 18: Fractional release of ^{90}Sr from HFR-K6/3

Particle failures were observed, from krypton release measurements, to have only occurred during the final 1800°C heating phase and this can be seen in the experimental data for the caesium curve in Figure 16. Low fractional releases are observed in the 1600°C and 1700°C heating phases followed by an increase occurs in the 1800°C phase. In the period of 11 years between the irradiation experiments and the heatup tests the radioactive silver data decayed and thus no silver measurements were possible. Strontium was not measured. Codes show good agreement with each other for all the radionuclides but all the codes overpredict the caesium release by an order of magnitude at the end of the experiment. Nevertheless, the codes agree qualitatively with the experimental results for caesium. The calculated silver release at the end of the experiment can be seen in Figure 17 to vary between 0.6 to 1.0.

5.6 *HFR-EU1bis*

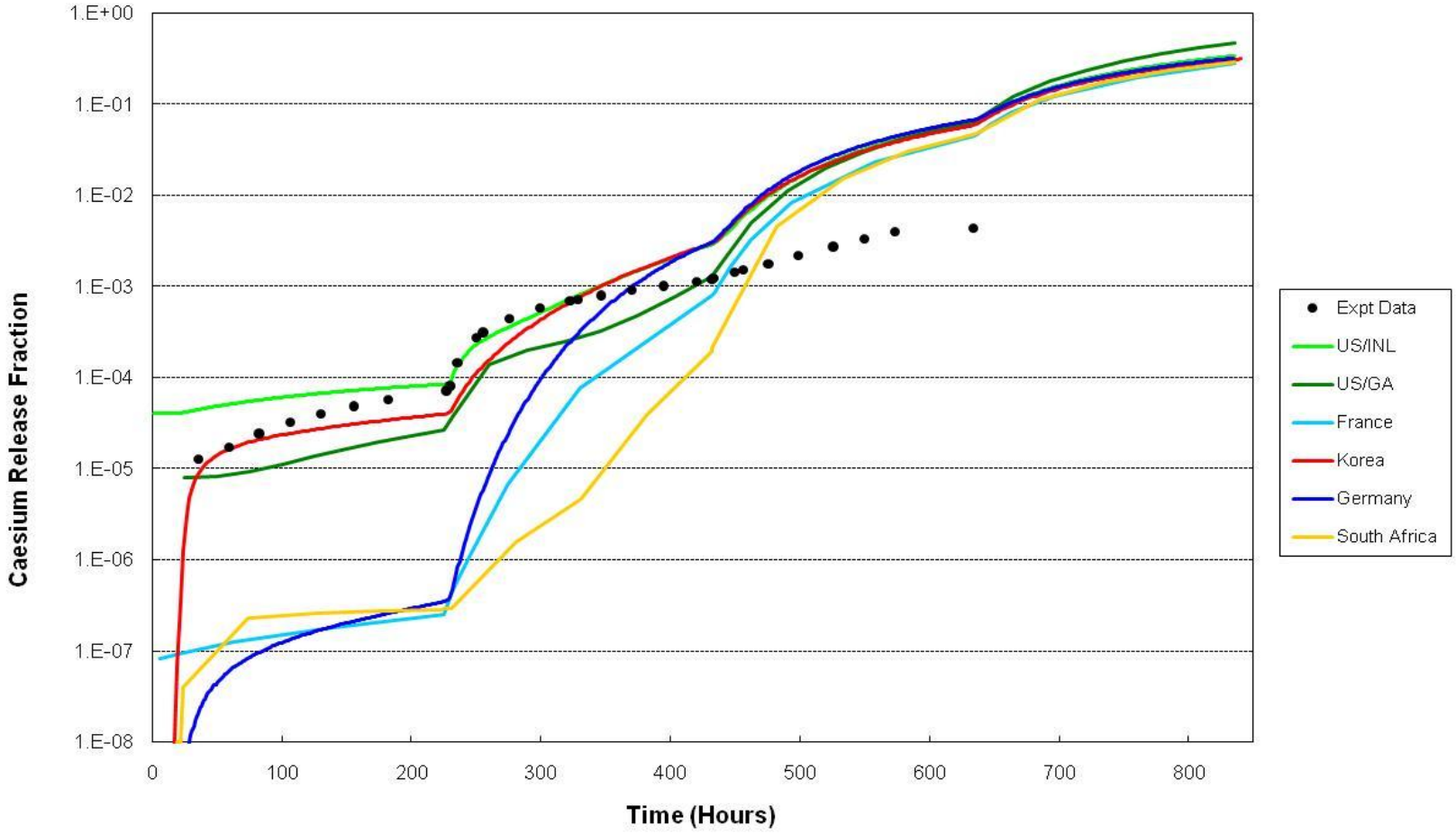

Figure 19: Fractional release of ^{137}Cs from HFR-EU1bis/1

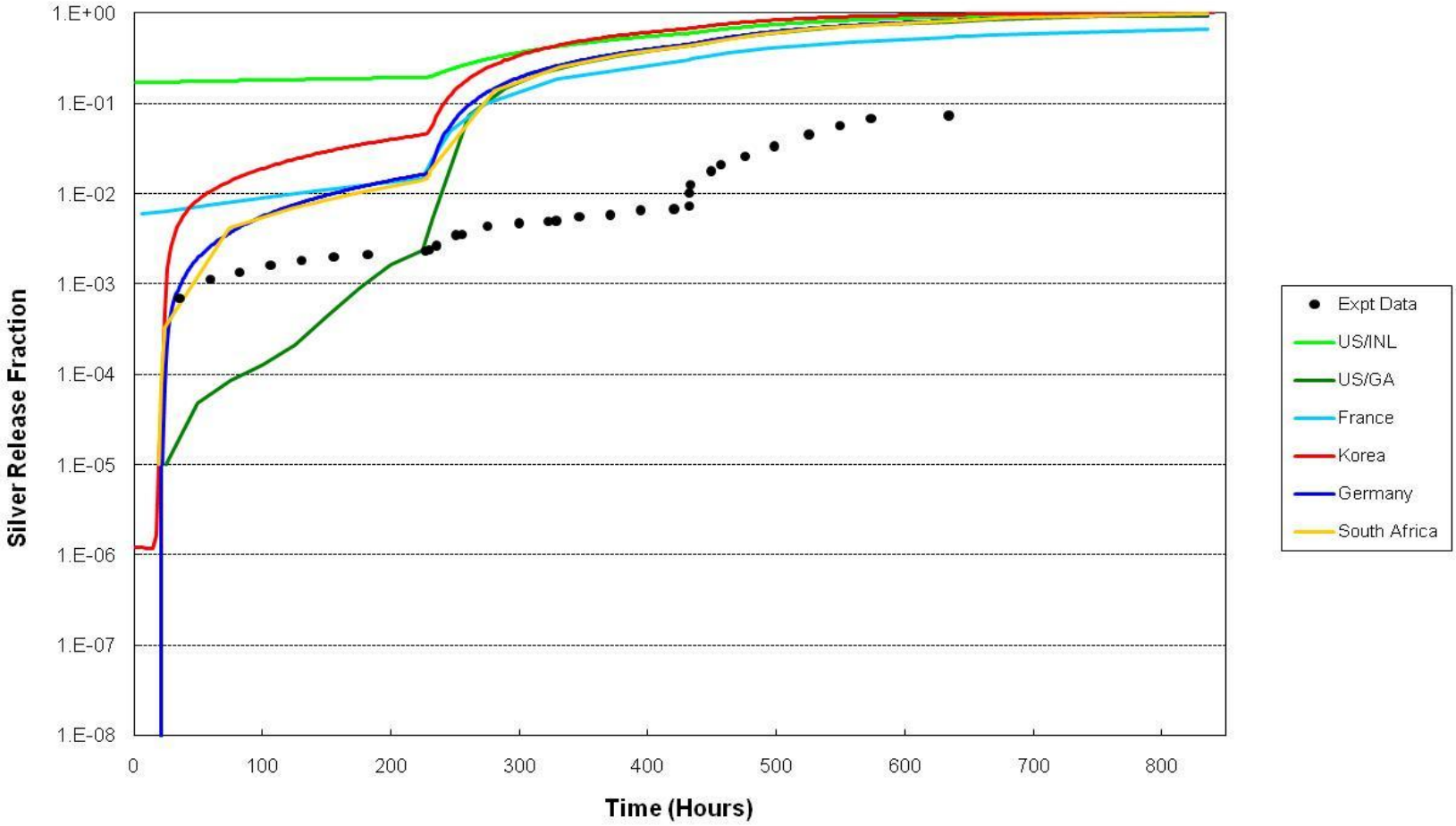

Figure 20: Fractional release of ^{110m}Ag from HFR-EU1bis/1

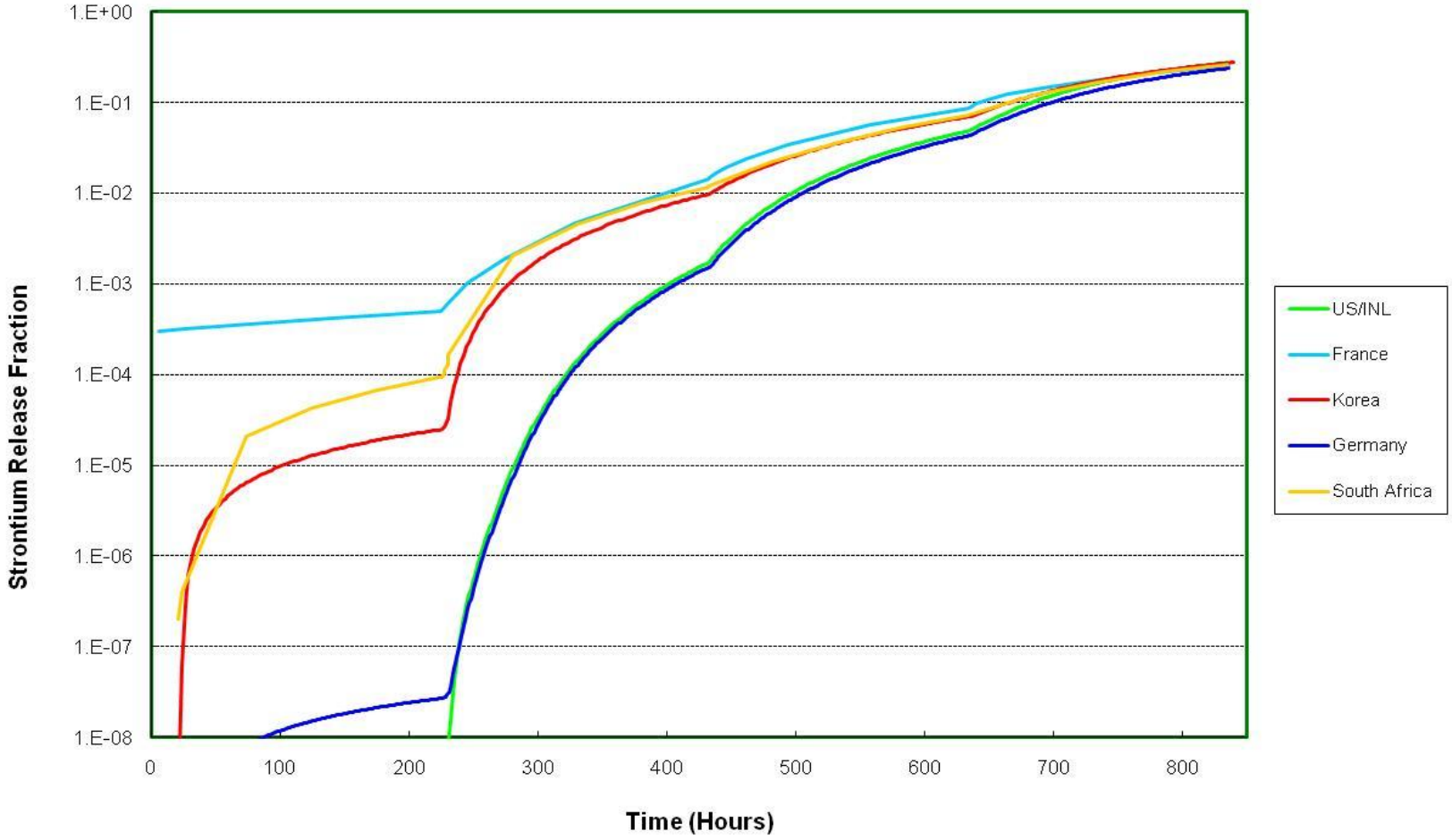

Figure 21: Fractional release of ^{90}Sr from HFR-EU1bis/1

For the caesium curve it can be seen that the codes and experimental results closely match during the heatup phases at 1250°C and 1600°C but differ during the 1700°C heating phase where the codes predict an order of magnitude higher release. This could be due to the fact that the codes model an almost instantaneous step up to a higher temperature, with a 2 hour delay in between, whereas in the experiment the fuel sphere was cooled down to room temperature after each heating phase and the cooldown and reheating took far longer than assumed by the codes. No experimental results are presented for the 1800°C heating phase as this was not performed.

5.7 *HTR-PM*

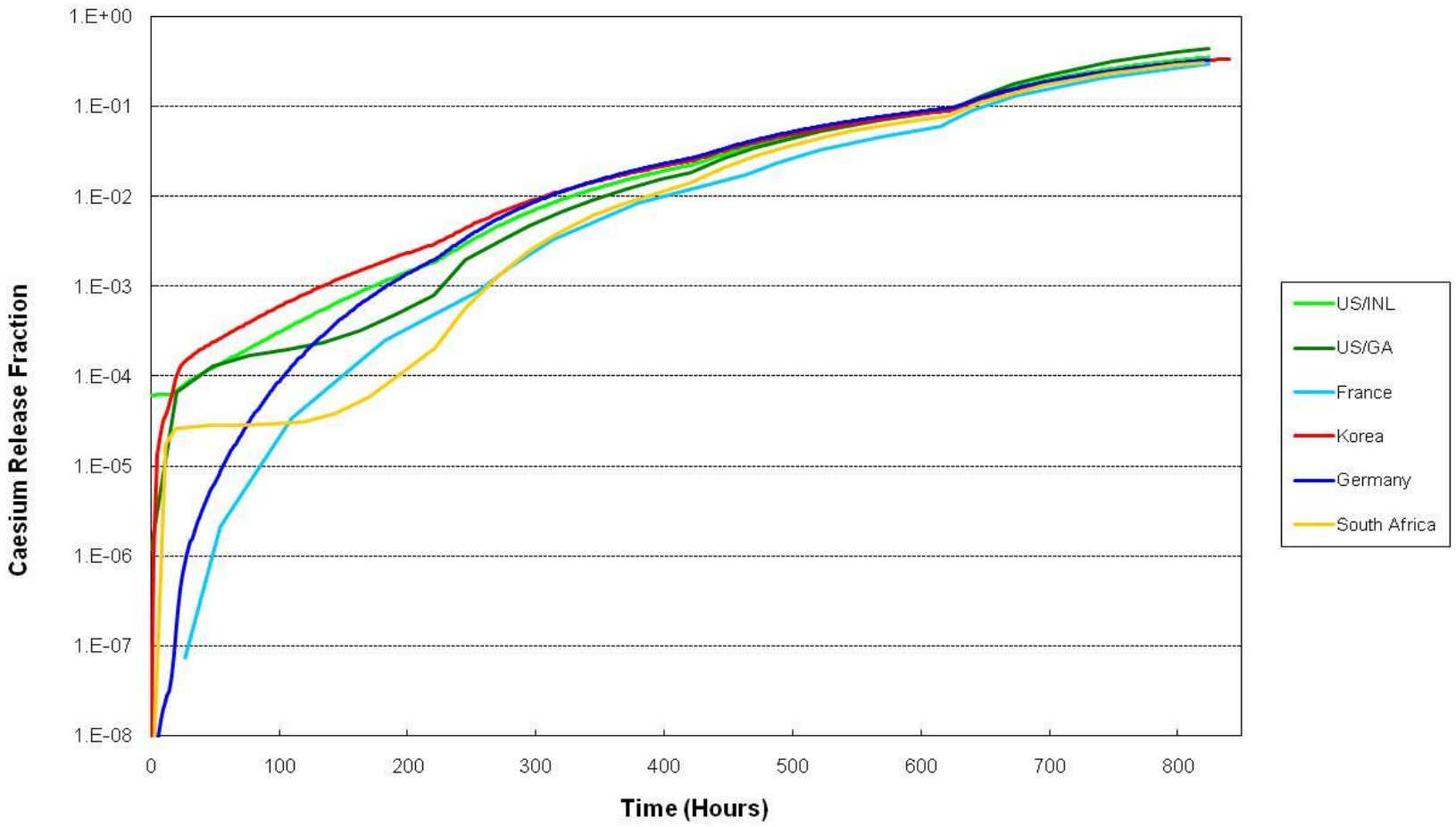

Figure 22: Fractional release of ^{137}Cs from the "HTR-PM" fuel sphere

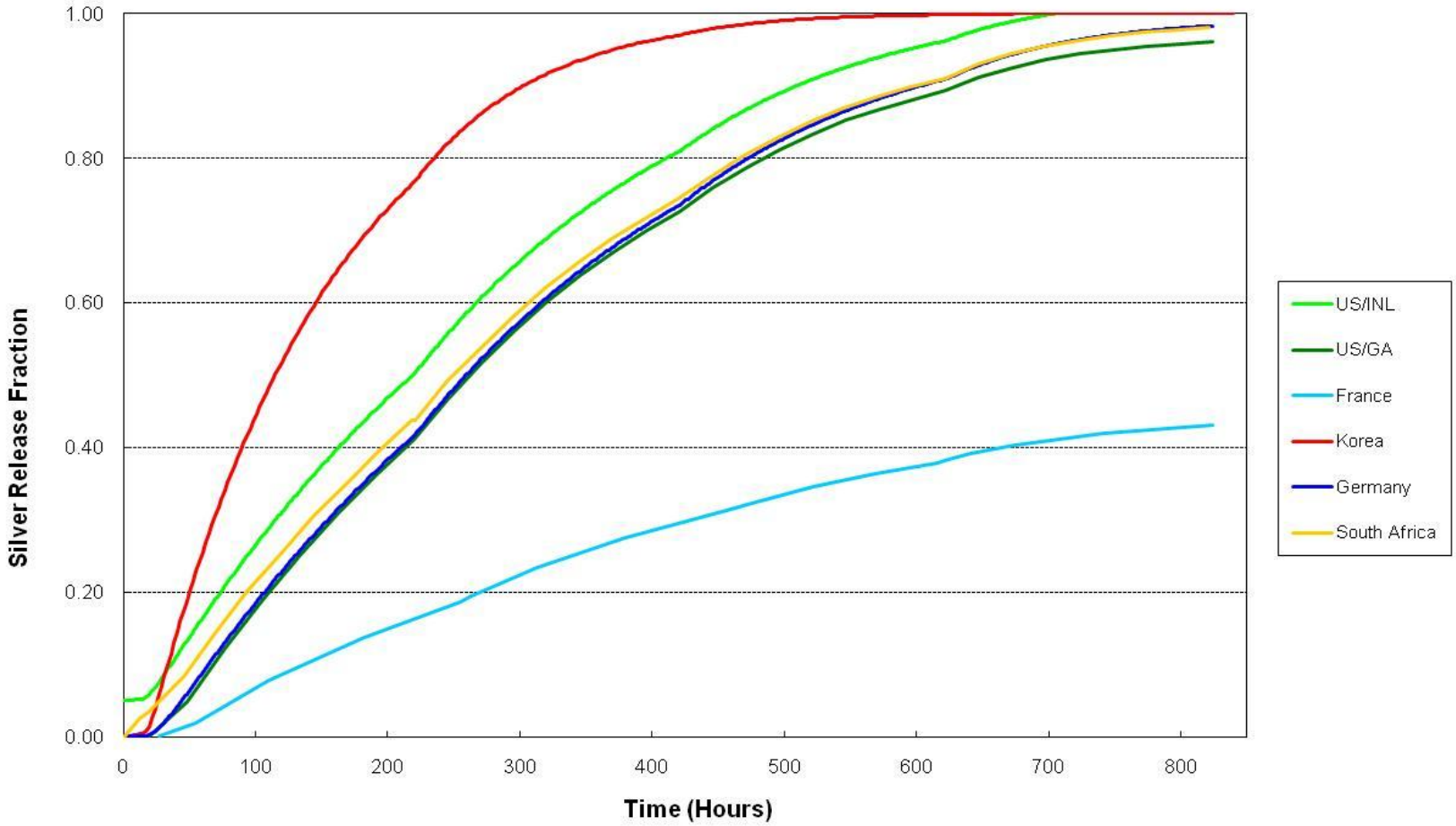

Figure 23: Fractional release of ^{110m}Ag from the "HTR-PM" fuel sphere

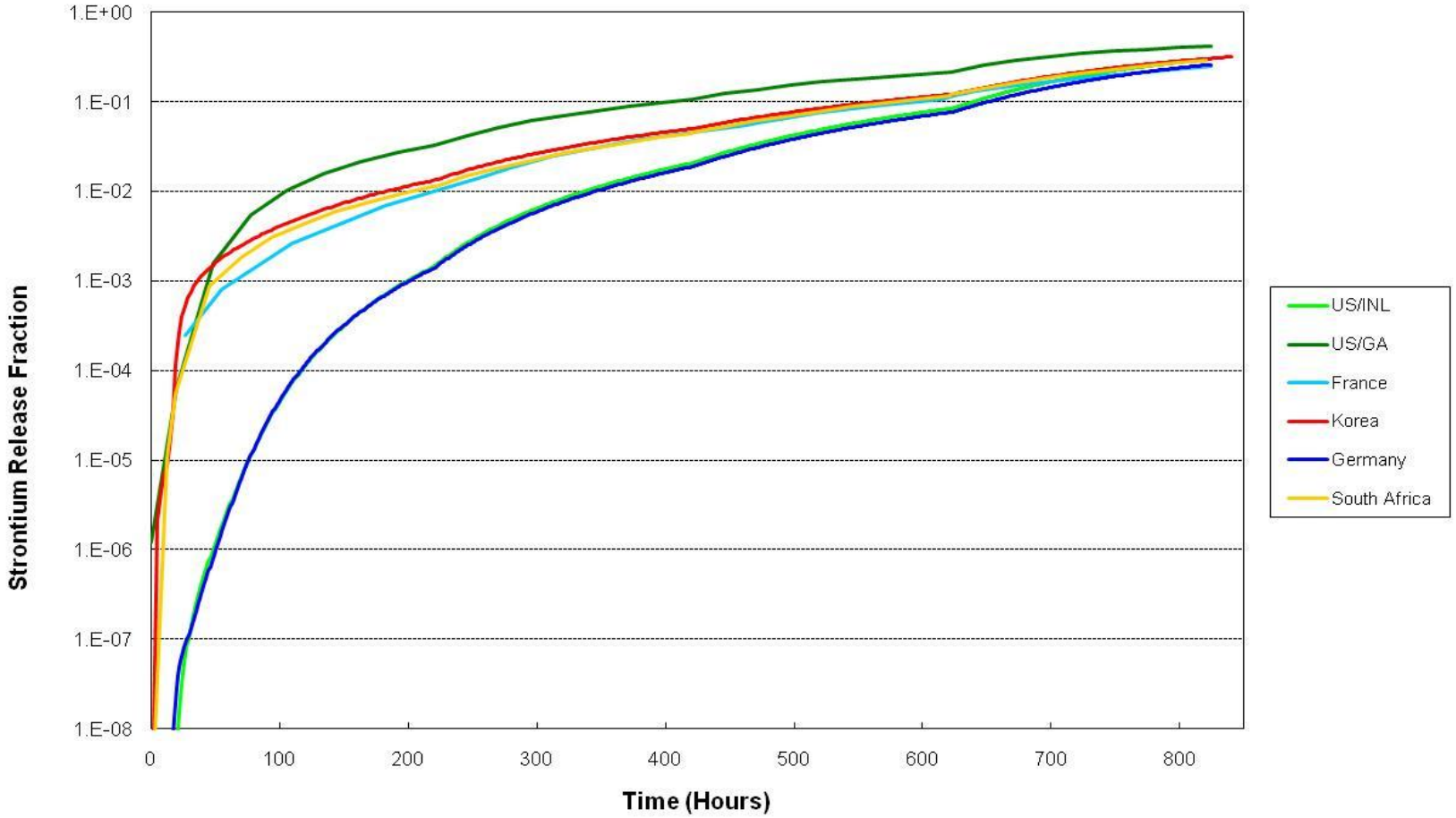

Figure 24: Fractional release of ^{90}Sr from the "HTR-PM" fuel sphere

For the HTR-PM case results are shown in **Figure 22** - Figure 24. It is seen that all codes show reasonable agreement.

6. Conclusion

An accident benchmark exercise such as this provides both a verification / validation function for codes but also gives input into further code development.

In terms of the sensitivity study the codes have shown good agreement taking into account the different assumptions used by the different codes.

For the irradiation and heatup tests caesium results appear to be the most predictable by the codes whilst strontium results are overpredicted by orders of magnitude and silver shows behaviour which is not consistent with a simple diffusion model. The strontium diffusion coefficient should be re-evaluated and the mechanisms for silver transport need to be investigated.

7. References

[1] ADAMS, C.C. 1988. Development of Improved TRISO-P Fuel Particle P-PyC Coating. General Atomics (**GA Report DOE/HTGR-88090**)

[2] BALDWIN, C. A. & KANIA, M.J. 1990. Fission Product Retention In TRISO Coated UO2 Particle Fuels Subjected To HTR Simulated Core Heating Tests. (In International Atomic Energy Agency Specialists Meeting on Behaviour of Gas Cooled Reactor Fuel under Accident Conditions held at Oak Ridge, Tennessee, USA on 5 and 7 November 1990. Vienna: International Atomic Energy Agency.)

[3] BRAMBLETT, G.C.; FISHER, C.R. & SWART, F.E. Operational experience at Fort St. Vrain. (In Proceedings of International Working Group on Gas-Cooled Reactors held in Lausanne on 1-3 September 1980. Lausanne)

[4] CARRÉ, F., YVON, P., LEE, W.J., Y. DONG, Y., TACHIBANA, Y. & PETTI, D. 2009. VHTR – Ongoing International Projects. (In Proceedings of GIF Symposium held in Paris on 9 and 10 September 2009. Paris. **p. 93 -102**).

[5] CHAROLLAIS, F.; BAKKER, K.; OBRY, P.; SHIHAB, S.; GUILLERMIER, P.; ABRAM, T; WERNER, H; KISSANE, M; TOSCANO, E.H.; FUETTERER, M. 2006. High-Temperature Reactor Fuel Technology in the European Projects HTR-F1 and RAPHAEL. (In Proceedings of 3rd International Topical Meeting on High Temperature Reactor Technology held in Johannesburg on 1 – 4 October 2006. Johannesburg.).

[6] CRANK, J. 1975 The Mathematics of Diffusion. Bristol: Oxford University Press. 424p.

[7] EVERETT III, J.L., & KOHLER, E.J., 1978. Peach Bottom Unit No. 1: A High Performance Helium Cooled Nuclear Power Plant. Annals of Nuclear Energy. 5(8-10):321-335.

[8] FUTTERERA, M.A, BERGA,G., MARMIER, A., TOSCANO, E.H., FREIS, D., BAKKER, K. & DE GROOT S. 2008. Results of AVR fuel pebble irradiation at increased temperature and burnuo in the HFR Petten. *Nuclear Engineering and Design*. 238(2008):2877–2885, November.

[9] HANSON, D. L. 2004. A Review of Radionuclide Release from HTGR Cores during Normal Operation. Electric Power Research Institute. (**EPRI Report 1009382.**).

[10] INTERNATIONAL ATOMIC ENERGY AGENCY (IAEA). 2009. Status and Prospects for Gas Cooled Reactor Fuels - Proceedings of two IAEA meetings held

in June 2004 and June 2005. Vienna: International Atomic Energy Agency. (**IAEA-TECDOC-CD-1616**).

[11] INTERNATIONAL ATOMIC ENERGY AGENCY (IAEA). 2010. High Temperature Gas Cooled Reactor Fuels and Materials. Vienna: International Atomic Energy Agency. 182p. (**IAEA-TECDOC-1645**).

[12] KAZUHIRO, S.; TSUTOMU, T. 2003. Investigation of irradiation behavior of SiC-coated fuel particle at extended burnup. *Nuclear Technology*. 142(3):250-259, June.

[13] KESHAW, J.B., VAN DER MERWE, J.J. 2006. GETTER—a model for fission product release from spherical HTR fuel elements. (In Proceedings of 3rd International Topical Meeting on High Temperature Reactor Technology held in Johannesburg on 1 – 4 October 2006. Johannesburg).

[14] KIM, Y.M. & CHO, M.S. 2008. Development of a Fission Product Release Analysis Code COPA-FPREL. (In Proceedings of International Conference on. Advances in Nuclear Power Plants (ICAPP-05) held in Seoul on 15 – 19 May 2005. Seoul).

[15] KOSTER, A., MATZIE, R. & MATZNER, D. Pebble-bed modular reactor: a generation IV high-temperature gas-cooled reactor. Proceedings of the Institution of Mechanical Engineers, Part A: Journal of Power and Energy. 218(5):309-318, September.

[16] H. KROHN & R. FINKEN. 1983. FRESCO-II: Ein Rechenprogramm zur Berechnung der Spaltproduktfreisetzung aus kugelförmigen HTR-Brennelementen in Bestrahlungs- und Ausheizexperimenten. (A code to calculate the fission product release from spherical HTR fuel elements in irradiation and heating experiments, in German). Jülich Research Center Internal Report. (**Jül-Spez-212**).

[17] MILLER, G.K., PETTI, D., VARACALLE, D.J. & MAKI, J.T. 2001. Consideration of the Effects on Fuel Particle Behavior from Shrinkage in the Inner Pyrocarbon Layer, *Journal of Nuclear Materials*. 295(2):205-212, June.

[18] MILLER, G.K., MAKI, J.T., KNUDSON, D.L. & PETTI, D. 2004. Current Capabilities Of The Fuel Performance Modeling Code PARFUME. (In Proceedings of 2nd International Topical Meeting on High Temperature Reactor Technology held in Beijing on 22 – 24 September 2004. Beijing).

[19] MINATO, K., SAWA, K., FUKUDA, K., BALDWIN, C.A., GABBARD, W.A., KIMBALL, O.F., MALONE, C.M., MONTGOMERY, F.C., MYERS, B.F. & PACKAN,

N.H. 1998. HRB-22 Capsule Irradiation Test for HTGR Fuel. Tokai-mura: Japan Atomic Energy Research Institute. (**JAERI Research 98-021**).

[20] NABIELEK, H., CONRAD, R., ROLLIG, K. & MEYERS B.F. Fuel Irradiation Experiments On HFRK6 and HFRB1 with Intermittent Water Vapour Injections. (In Proceedings of Technical committee meeting on response of fuel, fuel elements and gas cooled reactor cores under accidental air or water ingress conditions. Held in Beijing on 25-27 October 1993. Vienna: International Atomic Energy Agency. **IAEA-TECDOC-784**).

[21] NABIELEK, H., HICK, H., WAGNER-LOFTIER, M. & VOICE, E.H. 1974. Performance Limits of Coated Particle Fuel; Part III: Fission Product Migration in HTR Fuel. Dragon Project Report. (DP-828 (Part. 3)).

[22] NEXT BIG FUTURE, 2010. http://nextbigfuture.com/2010/02/current-status-and-technical.html. February 12, 2010.

[23] NUCLEAR ENERGY RESEARCH ADVISORY COMMITTEE (NERAC) & GENERATION IV INTERNATIONAL FORUM, 2002. Generation IV Roadmap: Description of Candidate Gas-Cooled Reactor Systems Report. (GIF-016-00).

[24] O'CONNOR, T.J., 2009. Gas Reactors – A Review of the Past, an Overview of the Present and a View of the Future. (In Proceedings of GIF Symposium held in Paris on 9 – 10 September 2009. Paris).

[25] PHÉLIP, M., MICHEL, F. PELLETIER, M., DEGENEVE, G. & GUILLERMIER, P. 2004. The ATLAS HTR Fuel Simulation Code Objectives, Description and First Results. (In Proceedings of 2nd International Topical Meeting on High Temperature Reactor Technology held in Beijing on 22 – 24 September 2004. Beijing).

[26] POWER ENGINEERING INTERNATIONAL, 2010. http://www.powergenworldwide.com/index/display/articledisplay/6322207443/articles/power-engineering-international/volume-18/Issue_3/regulars/world-news/INTERNATIONAL.html. 1st March 2010.

[27] RICHARDS, M. 1993. CAPPER. Coated Fuel Particle Irradiation Analysis. General Atomics Internal Report. (**UN94135576**).

[28] ROLLIG, K. 1977. Release of rare fission gases from spherical elements with coated fuel particles. *Nuclear Technology*. 35(2): 517–523, September.

[29] ROLLIG, K. 2001. Rechenprogram GETTER. (**WER Report GBRA 052 477**).

[30] SCHENK, W., GONTARD, R. & NABIELEK. H. 1994. Performance of HTR fuel samples under high-irradiation and accident simulation conditions, with emphasis on test capsules HFR-P4 and SL-P1. Forschungszentrum Jülich Internal Report.

[31] SCHENK, W., POTT, G. & NABIELEK, H. 1990. Fuel accident performance testing for small HTRs. *Journal of Nuclear Materials*. 171(1):19-30, April.

[32] SCHWARZ, D., BAUMER,R. 1998. THTR operating experience. *Nuclear Engineering and Design*. 109(1-2): 199-205, September – October.

[33] STAWICKI, M.A., 2006. Benchmarking of the MIT High Temperature Gas-Cooled Reactor TRISO-Coated Particle Fuel Performance Model. Cambridge, MA: Massachusetts Institute of Technology. (Dissertation - M.Sc.) 133p.

[34] TOSCANO, E.H., KOSTECKA, H, EJTON, J. & DE WEERD W. 2004. Post-Irradiation Testing of HTR-Fuel Elements under Accident Conditions, Part 1 and 2. (In Proceedings of 2nd International Topical Meeting on High Temperature Reactor Technology held in Beijing on 22 – 24 September 2004. Beijing).

[35] VAN DER MERWE J.J. 2004. Verification and Validation of the PBMR Models and Codes Used to Predict Gaseous Fission Product Release From Spherical Fuel Elements. Johannesburg: Rand Afrikaanse Universiteit. (Dissertation - M.Sc.) 127p.

[36] VAN DER MERWE, J.J. 2004. Development and validation of fission product release models and software at PBMR. (In Proceedings of 2nd International Topical Meeting on High Temperature Reactor Technology held in Beijing on 22 – 24 September 2004. Beijing).

[37] VAN DER MERWE, J.J., VENTER, J.H. 2006. HTR fuel design, qualification and analyses at PBMR. (In Proceedings from the American Nuclear Society's Topical Meeting on Reactor Physics, PHYSOR 2006, held in Vancouver on 10-14 September 2006. Vancouver).

[38] VERFONDERN, K. 1997. Fuel performance and fission product behaviour in gas-cooled reactors. Vienna: International Atomic Energy Agency. (**IAEA-TECDOC-978**).

[39] VERFONDERN, K. In Press. Advances in HTGR Fuel Technology. Vienna: International Atomic Energy Agency.

[40] VERFONDERN, K., LEE Y-W. 2005. Advances in HTGR Fuel Technology – A New IAEA Coordinated Research Program. (In Proceedings of International

Conference on. Advances in Nuclear Power Plants (ICAPP-05) held in Seoul on 15 – 19 May 2005. Seoul).

[41] VERFONDERN, K., NABIELEK, H. & KENDALL, J.M. 2007. Coated Particle Fuel for High Temperature Gas Cooled Reactors. *Nuclear Engineering and Technology*. 39(5):603-616, October.

[42] ZIERMANN, E. 1990. Review of 21 years of power operation at the AVR experimental nuclear power station in Jülich. *Nuclear Engineering and Design.* 121(2):135-142, July.